

OHSTPY-HEP-T-01-019  
hep-th/0109154

# AdS/CFT duality and the black hole information paradox

Oleg Lunin and Samir D. Mathur

Department of Physics,  
The Ohio State University,  
Columbus, OH 43210, USA

## Abstract

Near-extremal black holes are obtained by exciting the Ramond sector of the D1-D5 CFT, where the ground state is highly degenerate. We find that the dual geometries for these ground states have throats that end in a way that is characterized by the CFT state. Below the black hole threshold we find a detailed agreement between propagation in the throat and excitations of the CFT. We study the breakdown of the semiclassical approximation and relate the results to the proposal of gr-qc/0007011 for resolving the information paradox: semiclassical evolution breaks down if hypersurfaces *stretch* too much during an evolution. We find that a volume  $\mathcal{V}$  stretches to a maximum throat depth of  $\mathcal{V}/2G$ .

# 1 Introduction.

One of the most puzzling paradoxes in physics is the black hole information paradox. When black holes form and evaporate, the Hawking radiation appears to be correctly given by a semiclassical calculation, but the radiation so computed destroys unitarity and thus violates the principles of quantum mechanics. String theory has made substantial progress in understanding the quantum physics of black holes, and its results suggest very strongly that the evaporation process maintains unitarity (see for example [1, 2] and references therein). But there is no clear understanding of the mechanism by which the information manages to leak out of the black hole via the radiation.

The essential strength of the information paradox lies in the fact that Hawking's semiclassical calculation of the radiation is independent of any details of quantum gravity at small scales [3]. Thus even though we find in string theory many perturbative and nonperturbative quantum gravity effects at the Planck scale and string scale, it is unclear how to use them to effect the information transfer. It is plausible that the effects that correct the semiclassical computation are nonlocal, and finding them will involve fundamental changes in our understanding of when semiclassical gravity is valid.

We will work with the D1-D5 system. For this case the microscopic entropy and low energy radiation rates agree with the Bekenstein entropy and Hawking radiation of the corresponding black hole, including numerical factors [4, 5, 6, 7]. Such agreements contributed to Maldacena's remarkable conjecture [8] that the CFT describing the brane system is *dual* to the near horizon geometry produced by the branes. Though this AdS/CFT correspondence has been extensively studied, most of the analysis has pertained to the Neveu-Schwarz (NS) sector of the CFT, while the black holes in asymptotically flat spacetime arise in the Ramond (R) sector [9, 10]. (We will discuss this further below.) The ground state in the NS sector is unique, but in the R sector the ground state has a large degeneracy, so that a large number of microstates appear to correspond to the same geometry. This fact is not just a technical complication but an essential issue, since similar degeneracies yield the Bekenstein entropy of black holes.

In this paper we will analyze the AdS/CFT correspondence in the R sector. We find several agreements between microscopic quantities computed in the CFT (which we take to be a sigma model at the orbifold point) and the corresponding supergravity computations. The length scales emerging in these relations are quite different from those that are relevant for the analysis in the NS sector. The results indicate the way in which the semiclassical approximation may break down in string theory to allow information leakage in Hawking radiation.

## 1.1 Review of some basic issues

Consider first the classical geometry of D1 and D5 branes with no momentum charge and no angular momentum. At  $r \rightarrow \infty$  the geometry is flat, while at small  $r$  the geometry is locally  $AdS_3 \times S^3 \times M$  where the 4-manifold  $M$  is  $T^4$  or K3. We have a horizon at  $r = 0$ ,

and the part of  $AdS_3$  covered by the geometry is one ‘Poincare patch’. The direction  $y$  along the D1-branes is compactified on a circle of radius  $R$  when we wish to make a black hole in 5 dimensions, and this creates a periodic identification of points in the  $AdS$  space.

When we attempt to apply the AdS/CFT correspondence conjecture to this D1-D5 geometry we encounter several important questions:

(a) The Poincare patch of the AdS geometry smoothly extends past the horizon  $r = 0$  to the entire ‘global AdS’ spacetime. The complete geometry thus obtained has more than one asymptotically flat region [11]. But it appears strange if new spatial infinities could be created just by bringing together a (large but finite) number of branes in a normal spacetime with one asymptotic infinity.

One may argue that the semiclassical Poincare patch geometry stops short of the horizon  $r = 0$  because the identification  $y \rightarrow y + 2\pi R$  relates points that are closer and closer together as  $r \rightarrow 0$ . But this leads to the question: what is the effective value of  $r$  where we should end the geometry, and what happens when an incident wave reaches this value of  $r$ ? One may naively think that the critical value of  $r$  would correspond to the length of the  $y$  circle becoming order string length or Planck length. It was argued however in [12] that the geometry ends much further down the ‘throat’, and that the truncation of the throat is to be traced to the existence of nonzero angular momentum in the CFT state. We will discuss this issue in more detail in this paper.

(b) The D1-D5 bound state has a large degeneracy; the number of ground states is  $\sim e^{2\sqrt{2}\pi\sqrt{n_1 n_5}}$ , where  $n_1$  and  $n_5$  give the number of D1 and D5 branes. The metric of the Poincare patch appears to be the same for all these states. This is of course a version of the standard ‘black holes have no hair’ problem. One could try to argue that the branes sit at  $r \sim 0$  and thus carry information about the microstate. But this would contradict our expectation from the AdS/CFT duality: the duality suggests that the entire AdS region is already a dual description of the state of the branes, and we should not find the branes to be present at the end of the ‘throat’. (We will in fact argue below that no branes need be included at the end of the throat; rather the way that the throat ends characterizes the microstate.)

### **The difference between NS and R sectors.**

The initial proposal by Maldacena of the AdS/CFT correspondence [8] was motivated partly by results on black holes, and pertained to the near horizon geometry produced by branes in asymptotically flat spacetime. When we wrap D1, D5 branes on a circle  $y$  in spacetime, then the behavior of the fermions in the CFT is induced from the behavior of fermionic fields in the bulk. Since the supergravity in the bulk has fermions periodic around  $y$ , the D1-D5 CFT also has fermions that are periodic around the  $y$  circle, so the CFT is in the R sector. (If we put the fermions in the bulk supergravity to be antiperiodic

around  $y$  then the vacuum energy is nonzero, and flat spacetime ceases to be a solution. Since we want asymptotically flat spacetime, we will not consider this situation.)

The proposal in [8] did not however give an explicit way to relate correlators via the duality. The map of chiral operators and correlators was carried out by Gubser, Klebanov, Polyakov [13] and by Witten [14]. Let us analyze these and other approaches to AdS correlators, keeping in mind that we are interested in the following essential physics. A wave traveling towards  $r = 0$  becomes one of shorter and shorter wavelength, due to the redshift between infinity and the small  $r$  region. The wave does not reflect back to larger  $r$  unless we have some explicit modification to the physics of the ‘throat’. This monotonic infall of an incident quantum to the horizon is an essential aspect of the black hole problem; the particle itself does not appear to return but the deformation it creates in the geometry causes Hawking radiation to be emitted, and this radiation appears to carry no information about the infalling quantum.

In the analysis of Witten [14] the AdS space was rotated to Euclidean signature. This causes the Poincare patch to become a smooth space with no singularity at  $r = 0$ . However at the same time we lose the physics of the horizon; we cannot have traveling waves in Euclidean signature, nor do we have the accumulation of wavefronts near  $r = 0$  that signals the infall of the particle to the horizon. The situation is similar to rotating a black hole geometry to Euclidean signature: we get only the space outside the horizon, and the geometry is smooth at the location  $r = r_{horizon}$ . But with such a rotated geometry we cannot address the question of what happens to quanta that fall into the hole.

In [13] correlation functions were computed in the Poincare patch arising from the near horizon geometry of branes. The correlators were however computed for *spacelike* momenta  $p^2 > 0$ . The wavefunction in this case has a growing part and a decaying part at  $r = 0$ , and the growing part was set to zero to solve for the Green’s function. But real infalling particles have timelike or null momenta. The waveform is then oscillatory near  $r = 0$ , and we have no natural way to relate the ingoing and outgoing parts of the wave. (If we just drop the outgoing part, then we have particles being swallowed into the horizon, and we cannot make a Green’s function at the AdS boundary by using the propagator.)

Correlation functions have also been computed in the AdS geometry with Lorentzian signature and with arbitrary momenta, but in these calculations the spacetime was extended to the ‘global AdS’ space past  $r = 0$  [15]. To relate computations with this global AdS to the black hole question that we started with, we would have to connect the global AdS to asymptotically flat spacetime. It is unclear how this is to be done, especially if we wish to avoid the appearance of new asymptotically flat regions. As was mentioned above, it would be strange if matter falling onto the branes were to move smoothly through  $r = 0$  and emerge in a new asymptotically flat region, since we could make the brane geometry by gathering together branes in a spacetime which started with only one asymptotic infinity.

Thus we see that we cannot directly use any of the usual ways of computing correlators in the AdS/CFT correspondence to understand how information may return (as Hawking

radiation) after we throw some energy into the throat of the D1-D5 brane geometry. As mentioned before the difficulty is not just a technical issue, but rather the fact that if we could set up AdS correlators in a supergravity geometry that pertains to a black hole then we would directly observe information emerging in Hawking radiation. But extensive work with supergravity solutions have shown that we cannot get such a simple resolution of the black hole information problem; further the emerging Hawking radiation is a complicated multi-particle state even for a single high energy incident particle, so it makes sense that we are unable to compute simple 2-point functions in AdS that correspond to returning a particle from  $r = 0$ .

To address the black hole information problem we need to work in the R sector of the CFT, with Lorentzian signature, an asymptotically flat infinity, and with quanta that have timelike or null momenta. The global AdS geometry corresponds to the NS sector of the CFT; we must instead use the Poincare patch and try to resolve the physics at  $r = 0$ . Changing any of these conditions bypasses the information problem, even though we may get interesting AdS/CFT correspondence theorems.

## 1.2 Results

(A) We start by listing the R ground states of the D1-D5 CFT. These states may be represented pictorially in terms of the ‘effective string’, which has total winding number  $n_1 n_5 \equiv N$  around the  $y$  circle. In a generic state the effective string is broken up into a number  $m$  of ‘component strings’; each component string is wrapped  $n_i$  times around  $y$  before closing on itself, and  $\sum_i n_i = N$ .

Naively, the geometry of the D1-D5 supergravity solution appears to have a uniform throat (in the sense that that angular  $S^3$  asymptotes to a constant radius), all the way down to a horizon at  $r = 0$ . We find however that the throat ends at some point before  $r = 0$ . There is a singularity at the end of the throat characterized by a curve in 4-d space. The location and shape of this curve mirrors the CFT microstate. In the special case that the curve is a circle we recover the metrics of [16].

(B) If the throat extended all the way down to  $r = 0$  then throwing even an infinitesimal energy into the throat would lead to horizon formation at some value of  $r$ . Since the throat is actually finite, there is an energy scale  $\Delta E_{threshold}$  below which we can study matter quanta moving in the throat without formation of a horizon (this is the ‘hot tube’ studied in [12]).

Below the threshold of black hole formation  $\Delta E_{threshold}$  we construct a detailed map between the throat geometry and the dual CFT effective string. A quantum placed in the throat bounces several times up and down the throat before escaping to infinity; let the time for each bounce be  $\Delta t_{SUGRA}$ . In the dual CFT this quantum is represented by a set of left and a set of right movers on the effective string; these vibration modes travel around the string and meet each other at intervals  $\Delta t_{CFT}$ . For the special metrics of [16] we can separate the wave equation and obtain  $\Delta t_{SUGRA}$  precisely [12]. We find

(i)  $\Delta t_{CFT} = \Delta t_{SUGRA}$

(ii) The probability per unit time for the quantum to escape from the supergravity throat exactly equals the probability per unit time for the vibration modes on the effective string to collide and emerge as a graviton.

We then proceed to argue that even though we cannot solve the wave equation for a general microstate, we still get  $\Delta t_{CFT} \sim \Delta t_{SUGRA}$  for all microstates.

Note that the scale  $\Delta t_{SUGRA}$  is much larger than the radius of the  $AdS_3$  which appears in  $AdS/CFT$  computations of correlation functions performed in the NS sector [13, 14, 17]; thus we are probing a different set of quantities than are usually studied with the duality. Also note that in comparing emission rates we are using explicitly the part of spacetime that joins the near horizon geometry to flat space.

(C) In setting up the map between quanta in the supergravity throat and vibration modes of the CFT component strings we find the following: the naive map breaks down if we are forced to put more than one set of vibration modes on the same component string. In general the CFT state has several component strings, and we can thus describe several quanta in the supergravity throat. Interestingly, when we put enough quanta that we would run out of component strings in the CFT, we find on the supergravity side that we reach the threshold  $\Delta E_{threshold}$  for black hole formation.

At this point we note a close similarity of these results with a conjecture made in [18]. In [18] it was argued that to resolve the black hole information paradox we need spacetime to have the following property: semiclassical propagation on the spacetime breaks down if during the course of evolution an initial slice in a foliation is *stretched* beyond a certain length. Thus spacelike slices need to be endowed not only with their intrinsic geometry but also with a ‘density of degrees of freedom’; if the stretching dilutes these degrees too much then nonlocal effects spoil the usual evolution equation.

We find that the number of component strings in the CFT state act like the density of degrees of freedom for the dual throat geometry – when space is stretched to give longer throats we also have fewer component strings. We characterize the ‘stretch’ of a volume  $\mathcal{V}$  by the time  $\Delta t$  to travel down and back up the throat. We then find the relation

$$\Delta t_{max} = \frac{\mathcal{V}}{2G_N^{(5)}} \quad (1.1)$$

## 2 R ground states in the CFT and dual metrics for a special family

### 2.1 The states in the CFT

We consider the bound states of  $n_1$  D1 branes and  $n_5$  D5 branes in IIB string theory. We set

$$N = n_1 n_5 \quad (2.1)$$

The D5 branes are wrapped on a 4-manifold  $M$ , and thus appear as effective strings in the remaining 6 spacetime dimensions.  $M$  can be  $T^4$  or K3. The D1 branes and the effective strings from the D5 branes extend along a common spatial direction  $x_5 \equiv y$ , and  $y$  is compactified on a circle of length  $2\pi R$ . The low energy dynamics of this system is a  $N=(4,4)$  supersymmetric 1+1 dimensional conformal field theory (CFT). The CFT has an internal R-symmetry  $SU(2)_L \times SU(2)_R \approx SO(4)$ . This symmetry arises from the rotational symmetry of the brane configuration in the noncompact spatial directions  $x_1, x_2, x_3, x_4$ . The group  $SU(2)_L$  is carried by the left movers in the CFT and the group  $SU(2)_R$  is carried by the right movers.

Consider this CFT at the ‘orbifold point’ [19, 20, 21, 22, 23]. Then the CFT is a 1+1 dimensional sigma model where the target space is the orbifold  $M^N/S_N$ , the symmetric product of  $N$  copies of the 4-manifold  $M$ . We are interested in the R sector ground states of this system (these will be states with no left or right moving excitations).

These R ground states can be obtained by first finding all the chiral primary fields in the NS sector, which are states with  $h = j_3, \bar{h} = \bar{j}_3$ . Spectral flow then maps these chiral primaries to ground states of the R sector. Spectral flow acts independently on the left and right movers, in the following way

$$\begin{aligned} h^R &= h^{NS} - j_3^{NS} + \frac{c}{24} \\ j_3^R &= j_3^{NS} - \frac{c}{12} \end{aligned} \tag{2.2}$$

The R ground states all have  $h = \bar{h} = \frac{c}{24}$ .

### 2.1.1 Chiral primaries in the NS sector.

The  $M^N/S^N$  orbifold CFT and its states can be understood in the following way. We take  $N$  copies of the supersymmetric  $c = 6$  CFT which arises from the sigma model with target space  $M$ . The vacuum of the theory is just the product of the vacuum in each copy of the CFT. In the orbifold theory we find twist operators  $\sigma_n$  [24, 25]. The copies  $1, 2, \dots, n$  of the CFT permute cyclically into each other  $1 \rightarrow 2 \rightarrow \dots \rightarrow n \rightarrow 1$  as we circle the point of insertion of  $\sigma_n$ . (The other copies are not touched, and we ignore them for the moment.) In this given twist sector there are operators with various values of  $j_3$ , but we are interested in those that are chiral operators. The chiral operator in this twist sector with lowest dimension and charge is termed  $\sigma_n^{-}$  [26] and has

$$h = j_3 = \frac{n-1}{2}, \quad \bar{h} = \bar{j}_3 = \frac{n-1}{2} \tag{2.3}$$

Each copy of the CFT has the  $SU(2)$  currents  $J^{(i)a}, \bar{J}^{(i)a}$ , where the index  $i$  labels the copies. Define

$$J^a = \sum_{i=1}^n J^{(i)a}, \quad \bar{J}^a = \sum_{i=1}^n \bar{J}^{(i)a} \tag{2.4}$$

Then we can make three additional chiral primaries from  $\sigma^{--}$ :

$$\begin{aligned}\sigma_n^{+-} &= J_{-1}^+ \sigma_n^{--}, & h = j_3 = \frac{n+1}{2}, & \bar{h} = \bar{j}_3 = \frac{n-1}{2} \\ \sigma_n^{-+} &= \bar{J}_{-1}^+ \sigma_n^{--}, & h = j_3 = \frac{n-1}{2}, & \bar{h} = \bar{j}_3 = \frac{n+1}{2} \\ \sigma_n^{++} &= J_{-1}^+ \bar{J}_{-1}^+ \sigma_n^{--}, & h = j_3 = \frac{n+1}{2}, & \bar{h} = \bar{j}_3 = \frac{n+1}{2}\end{aligned}\tag{2.5}$$

The chiral primaries  $\sigma_n^{--}, \sigma_n^{+-}, \sigma_n^{-+}, \sigma_n^{++}$  correspond respectively to the  $(0,0), (2,0), (0,2), (2,2)$  forms from the cohomology of  $M$ . Both  $T^4$  and K3 have one form of each of these degrees. We will not consider the chiral primaries arising from the other forms on  $M$ ; this will not affect the nature of the arguments that we wish to present.

The operator  $\sigma_1^{--}$  is just the identity operator in one copy of the  $c = 6$  CFT. Thus for the complete CFT made from  $N$  copies we can write the above chiral operators as

$$\sigma_n^{\pm\pm} [\sigma_1^{--}]^{N-n}\tag{2.6}$$

It is understood here that we must symmetrize the above expression among all permutations of the  $N$  copies of the CFT; we will not explicitly mention this symmetrization in what follows.

More generally we can make the chiral operators

$$\prod_{i=1}^k [\sigma_{n_i}^{s_i, \bar{s}_i}]^{m_i}, \quad \sum_{i=1}^k n_i m_i = N\tag{2.7}$$

where  $s_i, \bar{s}_i$  can be  $+, -$ . This gives the complete set of chiral primaries that result if we restrict ourselves to the above mentioned cohomology of  $M$ .

### 2.1.2 Ground states in the R sector.

In the state (2.7) the  $N$  copies of the  $c = 6$  CFT are naturally grouped into subsets of size  $n_i$ . The operation of spectral flow proceeds independently in each such subset. Thus consider a subset corresponding to the  $n$  copies linked by a twist  $\sigma_n^{s, \bar{s}}$ . For this subset we have  $c = 6n$  in the spectral flow relations (2.2). After the flow we get the charges

$$\begin{aligned}\sigma_n^{--} &\rightarrow j_3^R = -\frac{1}{2}, \quad \bar{j}_3^R = -\frac{1}{2} \\ \sigma_n^{+-} &\rightarrow j_3^R = \frac{1}{2}, \quad \bar{j}_3^R = -\frac{1}{2} \\ \sigma_n^{-+} &\rightarrow j_3^R = -\frac{1}{2}, \quad \bar{j}_3^R = \frac{1}{2} \\ \sigma_n^{++} &\rightarrow j_3^R = \frac{1}{2}, \quad \bar{j}_3^R = \frac{1}{2}\end{aligned}\tag{2.8}$$

In fact these 4 operators, after flowing to the R sector, join up to form a representation of  $SU(2)_L \times SU(2)_R$  with  $(j, \bar{j}) = (\frac{1}{2}, \frac{1}{2})$ . This can be seen by noting that  $J_{-1}^+$  in the NS sector flows to  $J_0^+$  in the R sector.



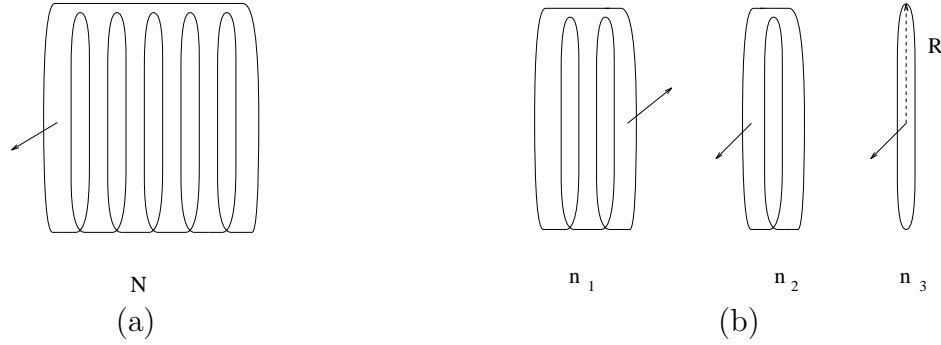


Figure 1: (a) The state with one component string wrapped  $n_1 n_5$  times around the direction  $y$ ; (b) A generic state with several component strings. The arrows indicate the spins of the component strings.

This treatment of each separate  $\sigma_n^{s,\bar{s}}$  would complete our treatment of the R ground state except for the fact that when we have more than one copy of the same operator then we must take only the symmetric combination of the different copies. Thus consider the set of chiral primaries (2.7) where the twist sector  $n$  occurs a total of  $m$  times, and concentrate attention on the  $nm$  copies of the  $c = 6$  CFT that are involved in these operators.

In the absence of symmetrization we would have, after flowing to the R sector, spin values  $(j, \bar{j}) = (\frac{1}{2}, \frac{1}{2})$  from each set (2.8), and we would add the spins according to the rules for SU(2) independently in the left and right SU(2)s. The symmetrization has the effect of giving, in the R sector, only the states with equal values of  $j_L$  and  $j_R$ :

$$\begin{aligned} (j, j^3; j, \bar{j}^3), \quad j &= \frac{m}{2}, \frac{m}{2} - 1, \dots, 0; & m \text{ even,} \\ j &= \frac{m}{2}, \frac{m}{2} - 1, \dots, \frac{1}{2}; & m \text{ odd.} \end{aligned} \quad (2.9)$$

(The values of  $j^3, \bar{j}^3$  range independently from  $-j$  to  $j$ .)

### 2.1.3 Pictorial description of R ground states.

The twist operator  $\sigma_N^{s,\bar{s}}$  joins all  $N$  copies of the  $c = 6$  CFT into one copy of the  $c = 6$  CFT (on an  $N$  times longer spatial circle). We depict the corresponding R ground state pictorially in figure 1 (a); we have a ‘multiwound’ string wrapped  $N = n_1 n_5$  times around the  $y$  circle. A generic state of the form (2.7) is pictured in figure 1(b); there are  $k$  ‘component strings’, with the  $i$ th string wrapped  $n_i$  times around the  $y$  circle.

Each component string carries spin  $(j_L, j_R) = (\frac{1}{2}, \frac{1}{2})$ , which we have depicted by the arrows on the component strings. We get a particularly simple set of geometries if all the spins are aligned (these geometries will be reviewed in the subsection below), but we will need to consider general spin orientations to address the physics of the generic microstate.

## 2.2 A special family of metrics for the D1-D5 system

Let us recall the physics of a special family of metrics for the D1-D5 system; these metrics were studied in [16, 12]. We will see in the next section that these special metrics correspond to CFT states arising from chiral primaries  $[\sigma_{N/m}^-]^m$ ; i.e., we have many component strings of equal length, and their spins are all aligned. The D1 and D5 charges are  $Q_1, Q_5$  respectively, and the angular momentum is specified by a parameter  $a$ . The 10-D metric and other supergravity fields are given in Appendix B, but for the most part we will need only the 6-D Einstein metric obtained by dimensional reduction on the 4-manifold  $M$ :

$$\begin{aligned} ds_E^2 = & -\frac{1}{h}(dt^2 - dy^2) + hf \left( d\theta^2 + \frac{dr^2}{r^2 + a^2} \right) - \frac{2a\sqrt{Q_1 Q_5}}{hf} (\cos^2 \theta dy d\psi + \sin^2 \theta dt d\phi) \\ & + h \left[ \left( r^2 + \frac{a^2 Q_1 Q_5 \cos^2 \theta}{h^2 f^2} \right) \cos^2 \theta d\psi^2 + \left( r^2 + a^2 - \frac{a^2 Q_1 Q_5 \sin^2 \theta}{h^2 f^2} \right) \sin^2 \theta d\phi^2 \right], \end{aligned} \quad (2.10)$$

where

$$f = r^2 + a^2 \cos^2 \theta, \quad h = \left[ \left( 1 + \frac{Q_1}{f} \right) \left( 1 + \frac{Q_5}{f} \right) \right]^{1/2} \quad (2.11)$$

This geometry is flat at spatial infinity. The direction  $y$  is assumed to be compactified on a circle of radius  $R$ . The size of the  $S^3$  in the variables  $\theta, \phi, \psi$  settles down to a constant for  $a \ll r \ll (Q_1 Q_5)^{1/4}$ , so we term the region  $r < (Q_1 Q_5)^{1/4}$  as a ‘throat’. Note however that since the  $y$  circle shrinks as  $r$  decreases, we will not in fact get a uniform throat if we dimensionally reduce along  $y$  and look at the 5-D Einstein metric. Thus we do not have a throat in the same sense as we get for the D1-D5-momentum system, but we continue to use the term ‘throat’ since it conveys the constancy of the  $S^3$  radius. The start of the throat is at  $r \sim (Q_1 Q_5)^{1/4}$ , but it is important that the throat is ‘capped off’ at  $r \sim a$ : the geometry ends smoothly except for a singularity on the curve  $r = 0, \theta = \pi/2$ .

Consider the massless scalar wave equation in the above metric. We can write the ansatz

$$\Phi(t, r, \theta, \phi, \psi, y) = \exp(-i\omega t + im\phi + in\psi + i\lambda y) \tilde{\Phi}(r, \theta). \quad (2.12)$$

It turns out however that there is an additional hidden symmetry in the metric, and there is a further separation between  $r$  and  $\theta$  [27].

In [12] the following process was studied. We start with a quantum of this scalar field at spatial infinity, sent in towards  $r = 0$ . Let the wavelength  $\omega^{-1}$  be much larger than the length scale  $(Q_1 Q_5)^{1/4}$ . Then most of the waveform reflects back to infinity from the start of the throat, but there is a small probability  $P$  for the quantum to enter the throat [28, 12]

$$P = 4\pi^2 \left( \frac{Q_1 Q_5 \omega^4}{16} \right)^{l+1} \left[ \frac{1}{(l+1)!l!} \right]^2 \quad (2.13)$$

where  $l$  specifies the spherical harmonic of the wave.

The part of the wave which enters the throat travels to  $r = 0$ , where it reflects back; we find naturally reflecting boundary conditions at the singularity. When the wave reaches back to the start of the throat we again have the same probability  $P$  that the quantum will escape to infinity, while the probability is  $1 - P \approx 1$  that it will reflect back into the throat. Thus the quantum travels several times in the throat before escaping. We can find the time for traveling once up and down the throat by looking at the phase shift between successive wavepackets emerging from the throat. This time is

$$\Delta t = \pi \frac{\sqrt{Q_1 Q_5}}{a}. \quad (2.14)$$

The parameter  $a$  is related to the angular momentum of the geometry as follows. The rotation group on the noncompact spatial directions is  $SO(4) \sim SU(2) \times SU(2)$ . The value of  $j$  in each  $SU(2)$  factor is the same, and it can be an integer or half integer. We have

$$a = \frac{2j}{n_1 n_5} \frac{\sqrt{Q_1 Q_5}}{R} \quad (2.15)$$

Following [16] we set

$$\gamma \equiv \frac{2j}{n_1 n_5} \quad (2.16)$$

The maximum value of  $j$  is  $\frac{n_1 n_5}{2}$ , so the maximum value of  $\gamma$  is unity.

Substituting (2.15) in (2.14) we get

$$\Delta t = \frac{\pi R}{\gamma} \quad (2.17)$$

### 3 CFT states and their dual supergravity throats

#### 3.1 Microscopic model used for black hole absorption computations.

We have seen in the past that absorption cross sections for D1-D5 black holes can be reproduced, including numerical factors, by the computation of absorption into the corresponding microstate. Let us briefly recall the nature of these microscopic computations.

The microstate was described by an ‘effective string’ wound  $N = n_1 n_5$  times around a circle; this circle is in the direction  $x_5 \equiv y$  and has length  $2\pi R$ . Among the various supergravity quanta that can be considered, the simplest are the s-wave ( $l = 0$ ) modes of minimally coupled scalars. Let the compact 4-manifold  $M$  be  $T^4$ , spanned by the coordinates  $x_6, x_7, x_8, x_9$ . Then the fluctuation  $h_{67}$  is an example of such a minimally coupled scalar, and we will use it for illustration in what follows.

When an incident quantum  $h_{67}$  encounters the effective string, its energy can get converted to that of vibrations of the string [5, 6, 40]. At low energies, the dominant process is the absorption of the s-wave, and this creates one left moving vibration quantum

and one right moving vibration quantum on the string. The incident quantum has an energy  $\omega$ , and its momentum lies only in the noncompact directions  $x_1, x_2, x_3, x_4$ . The vibrations of the string have momenta along  $x_5$ , and thus the energy momentum vectors are respectively for the left moving quantum and the right moving quantum

$$(p_0 = \omega/2, p_5 = -\omega/2) \quad \text{and} \quad (p_0 = \omega/2, p_5 = \omega/2) \quad (3.1)$$

Further, one of these vibrations is polarized in the direction  $x_6$  and the other is polarized in the direction  $x_7$ . The graviton in fact corresponds to the symmetric combination

$$h_{67} \rightarrow \frac{1}{\sqrt{2}} (|x_6\rangle_L \times |x_7\rangle_R + |x_7\rangle_L \times |x_6\rangle_R) \quad (3.2)$$

(The antisymmetric combination corresponds to absorption of the Ramond-Ramond 2-form  $B_{67}^{RR}$ .)

The amplitude for this absorption was computed in [6, 7] from the action for the effective string coupled to gravity. It was found that such a calculation with the effective string gave the same absorption cross section as that for absorption of low energy s-wave minimally coupled scalars into the D1-D5-momentum black hole. In [28] it was noted that this agreement persisted even if we do not have a large momentum charge, and in fact was also true to higher orders in the energy of the scalar as long as the D1 and D5 charges were kept large. This indicates that the simplest system that captures the effective physics would be the D1-D5 system with no momentum excitations; any momentum charge would be considered one of the possible excitations of our starting configuration. We will thus work with states of the D1-D5 system with no net momentum charge in this paper.

### 3.2 Time delay and its microscopic interpretation.

Let us first consider the state in the R sector that results from spectral flow of the chiral primaries

$$\sigma_N^{s, \bar{s}} \quad (3.3)$$

In this case the twist operator joins together all  $N = n_1 n_5$  strands of the effective string into one single ‘multiply wound’ strand, which was drawn schematically in figure 1(a).

This state corresponds to the string configuration used in [29, 6, 7, 28] in the study of black hole entropy and absorption. In our present considerations we will be also interested in the spin of this effective string. As discussed in the previous section, the variables  $s, \bar{s}$  take the values  $\pm \frac{1}{2}$ , and in the R sector the effective string forms a multiplet with

$$j_L = j_R = \frac{1}{2} \quad (3.4)$$

To study the picture of absorption by this effective string we have redrawn in figure 2 the string ‘opened up’ into a large circle; the length of this circle is  $2\pi R n_1 n_5$ . The incident

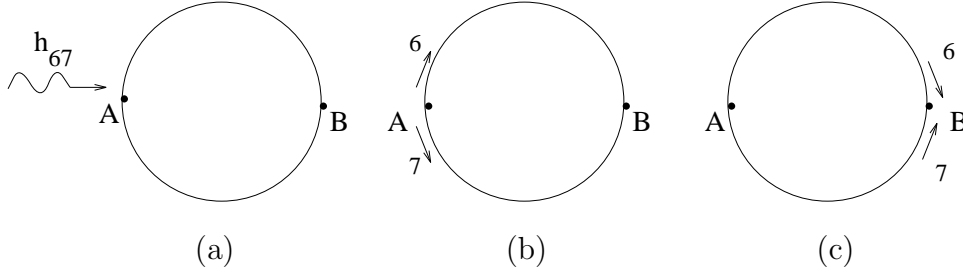


Figure 2: (a) A graviton is incident on the component string; (b) The graviton is converted to a pair of vibration modes; (c) The vibration modes meet again at B.

graviton  $h_{67}$  breaks up into a pair of vibration modes at the point marked  $A$ . Since the graviton had no momentum along the direction  $x_5 \equiv y$ , the amplitude for this process is the same for any position of the point  $A$  along the string. The wavefunction of the two vibration quanta is thus of the form

$$\Psi(y_1, y_2) = \psi(y_1 - y_2) \quad (3.5)$$

Here  $y_1, y_2$  are the coordinates of the left moving and right moving vibration modes on the effective string; thus  $0 \leq y_i < 2\pi R n_1 n_5$  in the present example. (We can think of these modes as massless open string states traveling along the effective string, and then  $y_1, y_2$  are the locations of these open strings.) The modes travel in opposite directions at the speed of light  $v = c = 1$ , and encounter each other again at the point  $B$  which is halfway along the effective string. The time interval between the start at  $A$  and the meeting at  $B$  is

$$\Delta t_{CFT} = \frac{2\pi R n_1 n_5}{2} = \pi R n_1 n_5 \quad (3.6)$$

As we will see below, there is only a small chance that the modes interact and re-emerge as a graviton at the point  $B$ . If they do not interact to leave the effective string, then they travel around again and re-encounter each other at the point  $A$ , after a further time (3.6).

As mentioned already there is nothing special about the points  $A, B$  on the string, since the center of mass of the two vibration modes is uniformly smeared over the string. The only physical quantity therefore is the time between successive encounters of the modes (not the place where they interact), and this time is given by (3.6).

Now let us look at the supergravity background corresponding to this R sector state. As summarized in the last section, the D1-D5 geometry with angular momentum  $j_L = j_R = j$  has a throat terminating after a certain distance. If a quantum of a minimally coupled scalar is incident from infinity, then there is a small probability that it enters the throat. If it does enter the throat, then it travels to the end where it reflects back and travels again to the start of the throat. Since the probability to enter the throat was small, the probability to leave the throat is also small, since these two probabilities are

equal. Thus the quantum travels several times up and down the throat before exiting the throat back to spatial infinity. The time for traveling once down the throat and back was computed in [12] and is given by (eqn. (2.17))

$$\Delta t_{SUGRA} = \frac{\pi R}{\gamma} = \frac{\pi R n_1 n_5}{2j} = \pi n_1 n_5 R \quad (3.7)$$

where we have used the fact that we have  $j = \frac{1}{2}$ .

This time  $\Delta t_{SUGRA}$  *exactly* equals the time  $\Delta t_{CFT}$  found in the microscopic computation in (3.6) above.

The essential idea of the AdS/CFT correspondence then yields the following picture:

(i) The effective string is dual to the throat region of the supergravity solution. It is important to note here that the throat is not infinitely long; otherwise we could not have found the above relation between  $\Delta t_{SUGRA}$  and  $\Delta t_{CFT}$ .

(ii) A graviton outside the throat in the supergravity solution is described by the graviton being present outside the effective string in the CFT picture. Note that we are working with quanta of wavelength  $\lambda$  much larger than the scale  $(Q_1 Q_5)^{1/4}$ , so this quantum outside the throat effectively travels in a flat metric in the supergravity solution.

(iii) The process where the quantum enters the throat in the supergravity solution maps to the process in the CFT where the incoming graviton converts its energy to that of the two vibration modes of the effective string. Similarly the process where the graviton manages to leave the throat and escape to infinity maps to the process in the CFT where the vibration modes collide and leave the effective string as a single graviton.

(iv) From (iii) above it is logical to identify the supergravity state where the quantum is near the start of the throat with the CFT configuration where the two vibration modes are close to each other, as at points  $A, B$  in figure 2. The quantum at the end of the throat (near  $r = 0$ ) maps to the CFT configuration where the vibration modes are separated by the maximal possible distance along the effective string. This is of course just a version of the UV/IR correspondence [30].

(v) The supergravity quantum travels several times up and down the throat, with a small probability to escape each time it reaches the start of the throat. Correspondingly, the vibration modes travel around the string, with a small probability to collide and leave the string as a graviton each time they meet.

In the following we will make this correspondence more precise, and provide additional evidence for the proposed relation between CFT excitations and their description in the supergravity dual.

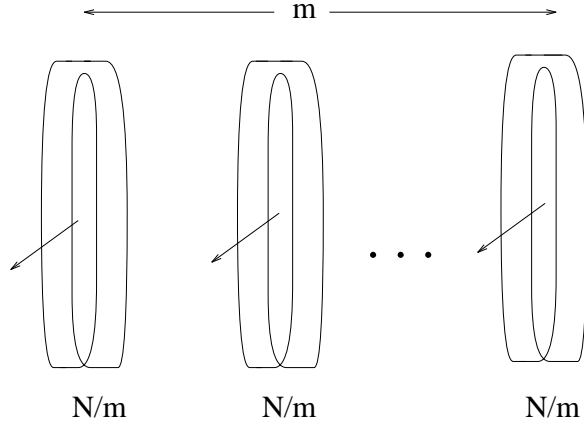


Figure 3: Component strings for the state  $[\sigma_{N/m}^{--}]^m$ . The spins are all aligned to give  $j = m/2$ .

### 3.3 General values of $j$ .

As we will see later in the section on black hole formation, for the case  $j_L = j_R = \frac{1}{2}$  considered above the supergravity solution is not trustworthy all the way to the end of the throat. More precisely, the backreaction of the quantum placed in the throat deforms the throat in a significant way, at least near the end of the throat. To avoid this we now look at larger values of angular momentum, where it will turn out that the backreaction of the quantum can indeed be ignored.

Let us look at a state of the CFT with

$$j_L = j_R = j = \frac{m}{2} \quad (3.8)$$

The simplest way to make such a state is to take the chiral primary in the NS sector

$$[\sigma_{\frac{N}{m}}^{--}]^m \quad (3.9)$$

Upon spectral flow to the R sector, each component  $\sigma_{\frac{N}{m}}^{--}$  gives a ‘multiwound’ string that is wound

$$n = \frac{N}{m} = \frac{n_1 n_5}{m} \quad (3.10)$$

times around the circle  $x_5 \equiv y$ . There are  $m$  such component strings. We sketch this configuration in figure 3. The spin of each multiwound component is  $j_L = j_R = \frac{1}{2}$ , and in the state that we have taken all these spins are aligned to produce the spin values (3.8).

An incident graviton can be absorbed into any of these  $m$  component strings. But now the travel time for the vibration modes around the string, before they meet each other again, is

$$\Delta t_{CFT} = \frac{\pi n_1 n_5 R}{m} \quad (3.11)$$

Now we look at the corresponding supergravity solution. When the angular momenta are given by (3.8) then the time for a quantum to travel once down and back up the throat is (eqn.(2.17))

$$\Delta t_{SUGRA} = \frac{\pi R}{\gamma} = \frac{\pi R n_1 n_5}{2j} = \frac{\pi n_1 n_5 R}{m} \quad (3.12)$$

Thus again we find

$$\Delta t_{CFT} = \Delta t_{SUGRA} \quad (3.13)$$

We have used the s-wave quanta as an illustration but we see immediately that we get the relation (3.13) for higher partial waves as well. The supergravity travel time  $\Delta t_{SUGRA}$  was found in [12] to be independent of the harmonic order  $l$ . In the CFT the absorption of a higher partial wave creates set of massless left movers  $\partial X \psi \dots \psi$  and a set of massless right movers  $\bar{\partial} X \bar{\psi} \dots \bar{\psi}$  [31, 33, 32]. Each set of excitations travels at the speed of light around the component string, so that  $\Delta t_{CFT}$  is independent of  $l$  as well.

### 3.4 The rate of radiation.

Suppose that we place an s-wave scalar quantum in the supergravity throat; the dual CFT state has a pair of vibration modes on the effective string. We wish to compute the probability per unit time for the scalar quantum to escape from the throat, and compare this to the probability per unit time for the vibration modes on the effective string to collide and leave the string.

First we look at the CFT computation. Let there be one left moving vibration and one right moving vibration on the string, with the momentum vectors (3.1) and in the wavefunction corresponding to a graviton (3.2). The interaction that leads to the emission of the graviton is given by using the DBI action for the effective string. The computation is essentially the same as that done for absorption into the black hole microstate, but since we are here looking at the emission rate we reproduce the relevant calculation in Appendix A. Consider the R ground state arising from the chiral primary  $[\sigma_{N/m}^-]^m$ . This state has  $m$  component strings, all in the same state, and the spins are aligned to give  $j_l = j_R = \frac{m}{2}$ . Then the probability per unit time for the vibrations to collide and emit a graviton is found to be

$$\mathcal{R}_{CFT} = m \frac{\pi^2 \omega^4 g^2}{2V(2\pi)R} \quad (3.14)$$

Here  $g$  is the string coupling,  $(2\pi)^4 V$  is the volume of the  $T^4$  and we have set  $\alpha' = 1$ .

Now we look at the supergravity solution. The throat is assumed to be long compared to the scale  $(Q_1 Q_5)^{1/4}$  of the geometry near the start of the throat. A quantum incident from infinity has a probability  $P$  to enter the throat, after which it propagates down the throat till it reaches the end where it reflects. The long length of the throat implies that the probability  $P$  depends only on the geometry near the start of the throat, which is the same as the geometry in the nonrotating case  $j = 0$ . Thus we can read this probability



off from [28, 12], and we find (using eqns (2.13), (B.4))

$$P = \frac{\pi^2}{4} Q_1 Q_5 \omega^4 = \frac{\pi^2}{4} \omega^4 \frac{n_1 n_5 g^2}{V} \quad (3.15)$$

The number of times the quantum tries to exit the throat per unit time is

$$\frac{1}{\Delta t_{SUGRA}} \quad (3.16)$$

Thus the probability of emission per unit time is (using (3.12), (3.15))

$$\mathcal{R}_{SUGRA} = \frac{P}{\Delta t_{SUGRA}} = m \frac{\pi^2}{2} \omega^4 \frac{g^2}{V} \frac{1}{2\pi R} \quad (3.17)$$

We see that

$$\mathcal{R}_{CFT} = \mathcal{R}_{SUGRA} \quad (3.18)$$

so that the rates of emission agree *exactly* between the supergravity and CFT pictures.

Let us compare the above calculation with the computations [6, 7, 28] that show agreement between microscopic radiation rates and Hawking radiation rates from the corresponding black holes. The CFT computation is the same in each case. But on the supergravity side in the present case we do not have a horizon, and the graviton does not represent Hawking radiation. We are in fact below the black hole formation threshold, and so instead of finding a horizon somewhere down the throat we find a point from which we can reflect back. The travel time  $\Delta t_{SUGRA}$  has no analogue if we have a horizon. Thus the agreement (3.18), while similar to that in the black hole case, has a somewhat different interpretation.

## 4 Generic microstates and the dual throat geometries

So far we have used specific examples of D1-D5 microstates to argue that  $\Delta t_{CFT} = \Delta t_{SUGRA}$ . For this to be a general principle, however, we must examine all possible R ground states of the D1-D5 system.

### 4.1 Unbound states: a potential difficulty and its resolution

A simple way to violate  $\Delta t_{CFT} = \Delta t_{SUGRA}$  would appear to be the following. Take two D1-D5 bound states, with angular momenta

$$(j_L = j_L^3 = \frac{m}{2}; j_R = j_R^3 = \frac{m}{2}) \quad \text{and} \quad (j_L = -j_L^3 = \frac{m}{2}; j_R = -j_R^3 = \frac{m}{2}) \quad (4.1)$$

Since such D1-D5 states are mutually BPS, we can construct a supergravity solution with arbitrary locations for the centers of the two parts. Let the two centers be coincident. The angular momentum of the two bound states cancel each other, so that we get  $j_L = j_R = 0$ . Naively, looking at eqn. (2.14), (2.15) one may think that this geometry will have an infinite throat and infinite  $\Delta t_{SUGRA}$ . But looking at the lengths of the component strings in the CFT we still find  $\Delta t_{CFT} = \frac{\pi n_1 n_5 R}{m}$ , so that we have a potential contradiction.

But a closer look at the supergravity solution reveals the following. The rotation parameter  $a$  in the solution (2.10) multiplies  $dt d\phi$ , but it also appears in the function  $f = r^2 + a^2 \cos^2 \theta$ . Suppose we take a solution (2.10) with rotation parameter  $a$  and superpose another solution with the same charges and rotation parameter  $\tilde{a} = -a$ , and the same center. Then the coefficient of  $dt d\phi$  disappears, but  $f$  remains unchanged since it does not depend on the sign of  $a$ . We have developed in Appendix C an extension of the chiral null models to yield directly general solutions for the D1-D5 system. The 6-D Einstein metric for this superposition, worked out in Appendix D, is

$$ds_E^2 = -\frac{f_0}{\sqrt{f_1 f_5}}(dt^2 - dy^2) + \sqrt{f_1 f_5} \left( \frac{dr^2}{r^2 + a^2} + d\theta^2 \right) + \frac{\sqrt{f_1 f_5}}{f_0} \left[ r^2 \cos^2 \theta d\psi^2 + (r^2 + a^2) \sin^2 \theta d\phi^2 \right] \quad (4.2)$$

where

$$f_0 = r^2 + a^2 \cos^2 \theta, \quad f_1 = f_0 + Q_1, \quad f_5 = f_0 + Q_5 \quad (4.3)$$

We cannot solve the wave equation in this metric since the variables do not separate. But we can estimate the time delay by looking at geodesics in the throat. A generic geodesic goes down the throat only down to  $r \sim a$ ; the travel time is then<sup>1</sup>

$$\Delta t_{SUGRA} \sim \Delta t_{CFT} \quad (4.4)$$

We can superpose several D1-D5 bound states, each having rotation but such that the combined angular momentum is zero. It is easy to generalize the above construction to see that in each case we still get  $\Delta t_{SUGRA} \sim \Delta t_{CFT}$ .

## 4.2 Arbitrary $j$ configurations of the bound state

Let us now return to our principal consideration – the analysis of a single D1-D5 bound state. Here again we face the following potential problem. Consider the R ground state that results from a chiral primary made of  $m$  components, each of the form  $\sigma_{N/m}^{s, \bar{s}}$ . If the spins  $s, \bar{s}$  are all aligned then we get  $j_L = j_R = \frac{m}{2}$ ; this is the maximum value of  $j$  in (2.9)

---

<sup>1</sup>There exist an exceptional set of geodesics that head directly into the singularity at  $r = 0, \theta = \pi/2$ , which do not return back in a finite time  $t$ . As we will note below (and this is explained in more detail in Appendix I) this situation is not generic; in a generic solution the geodesics (and waves) reflect back in a finite time from the singularity. We also argue in Appendix I that quantum fluctuations of the metric will result in  $\Delta t_{exceptional} \sim \Delta t_{CFT} \times \log j$  even for such nongeneric geometries.

and gives the configuration we studied in the section 3. But from (2.9) we see that we can also combine the spins  $s, \bar{s}$  to obtain states with lower  $j$ , all the way down to  $j \approx 0$ . Does the effective length of the throat depend on the value of  $m$  or on the value of  $j$ ? If it depends on  $j$  then we have a problem; by choosing  $m \gg 1$  we make the component strings of the CFT small (length  $\sim 2\pi RN/m$  each) but the supergravity throat could be made long by letting  $j \approx 0$ . We will see however that the supergravity throat terminates at a distance that depends on  $m$  rather than  $j$ . This fact will be crucial to our conjecture that  $\Delta t_{CFT} = \Delta t_{SUGRA}$ .

#### 4.2.1 The duality map from D1-D5 to FP

To see the nature of supergravity solutions corresponding to general values of  $j$  in (2.9) we will map the D1-D5 system by a chain of dualities to the FP system: F represents fundamental string winding (along  $x_5 \equiv y$ ) and P represents momentum (also along  $y$ ). The reason for starting the analysis with the FP system is the following. The  $M^N/S^N$  orbifold CFT describes a single D1-D5 bound state. To study the supergravity dual we need the metric for a single bound state system, and not for a superposition of many such bound states. In the FP language a single bound state is easy to characterize: it arises from a single multiwound string carrying left moving vibrations. Duality then maps such FP solutions to metrics of single D1-D5 bound states.

The sequence of dualities needed to map the D1-D5 system to the FP system is easy to write, and can be found for example in [34]. The following is the relation of quantities and states in the two systems:

(i) The number of D5-branes in the D1-D5 system becomes the winding number  $n_w$  of the fundamental string (i.e.  $n_w = n_5$ ). The number of D1-branes becomes the number of units of momentum ( $n_p = n_1$ ). The bound state of the D1-D5 system maps to a bound state of the winding and momentum modes of the FP system. Let the radius of the  $y$  circle after dualities be  $R'$ . The string of the FP system then has a total length  $L_T = 2\pi R' n_w$ . Momentum modes on this string come in fractional units

$$p = \frac{2\pi n}{L_T} = \frac{n}{n_w R'} \quad (4.5)$$

with the constraint that the total momentum has the form

$$P_T = \frac{n_p}{R'} = \frac{n_w n_p}{n_w R'} \quad (4.6)$$

with  $n_p$  an integer [35]. Thus on the fundamental string of total length  $L_T$  the total level number of excitations is

$$N = n_p n_w = n_1 n_5 \quad (4.7)$$

(ii) Let the fundamental string carry a quantum of vibration in a transverse direction  $i$ ,  $i = 1, 2, 3, 4$  with wavelength  $\lambda = L_T/n$ . This excitation is generated by the oscillator

$\alpha_{-n}^i$ . If the string has  $n_p = N/n_w$  units of momentum then the total state of the string is of the form

$$[\alpha_{-n_1}^{i_1}]^{m_1} \dots [\alpha_{-n_k}^{i_k}]^{m_k} |0\rangle \quad (4.8)$$

with

$$\sum_j m_j n_j = N \quad (4.9)$$

The state (4.8) corresponds in the D1-D5 system to the chiral primary

$$[\sigma_{n_1}^{s_1, \bar{s}_1}]^{m_1} \dots [\sigma_{n_k}^{s_k, \bar{s}_k}]^{m_k} \quad (4.10)$$

Thus in the R ground state of the D1-D5 system if we have a component string that is wound  $n$  times around  $y$  then this component string maps to a momentum mode  $\alpha_{-n}$ , which has wavelength  $L_T/n$  around the fundamental string in the FP system. The component string in the D1-D5 system has four polarization states  $(s, \bar{s}) = (\pm\frac{1}{2}, \pm\frac{1}{2})$  which gives the spins under  $SU(2)_L \times SU(2)_R = SO(4)$ , and these map to the four polarizations  $\alpha^i$  of the momentum mode.<sup>2</sup>

#### 4.2.2 Mapping D1-D5 states to FP configurations

Let us study the FP representation of some selected R ground states of the D1-D5 system.

(i) Take the chiral primary

$$[\sigma_n^{--}]^{N/n} \quad (4.11)$$

of the NS sector of the D1-D5 system and consider its corresponding R ground state. There are  $N/n$  component strings of winding number  $n$  each. Figure 4(a) depicts this state for  $n = 2$ .

In the FP system we have  $N/n$  quanta of the  $n$ th harmonic around the fundamental string. Further, since the spins of the factors in (4.11) are all aligned, the angular momentum is  $j_L = j_R = \frac{N}{2n}$ . The fundamental string rotates in a circle; the metric of this state and the duality maps were constructed in [34]. Let the rotation generators of the two  $SU(2)$  factors and the  $SO(4)$  be related such that  $j_L^3 = \frac{1}{2}(M_{12} + M_{34})$ ,  $j_R^3 = \frac{1}{2}(M_{12} - M_{34})$ ; then the choice  $(j_L^3, j_R^3) = (-\frac{1}{2}, -\frac{1}{2})$  for each  $\sigma_n$  in (4.11) implies that the rotation of the string is in the  $x_1$ - $x_2$  plane.

This F string is pictured in figure 4(b), opened up to its total length  $2\pi R' n_w = 2\pi R' n_5$ . Due to the identification  $y \rightarrow y + 2\pi R'$  the string actually covers a cylindrical surface in a helical fashion; this is pictured in figure 4(c). We can characterize this cylinder by its cross section, which is a circle, depicted in figure 4(d).

---

<sup>2</sup>The  $M^N/S^N$  orbifold does not include the center of mass  $U(1)$  factor of the D1-D5 system, so we see only one vacuum  $|0\rangle$  in (4.8) rather than all the ground states of a single fundamental string without momentum. Further we are concentrating on only those chiral primaries in the D1-D5 system that arise from the  $(0,0), (0,2), (2,0), (2,2)$  forms on the 4-manifold  $M$ , so we write only the polarizations  $\alpha^i$  for the momentum modes rather than all possible polarizations.

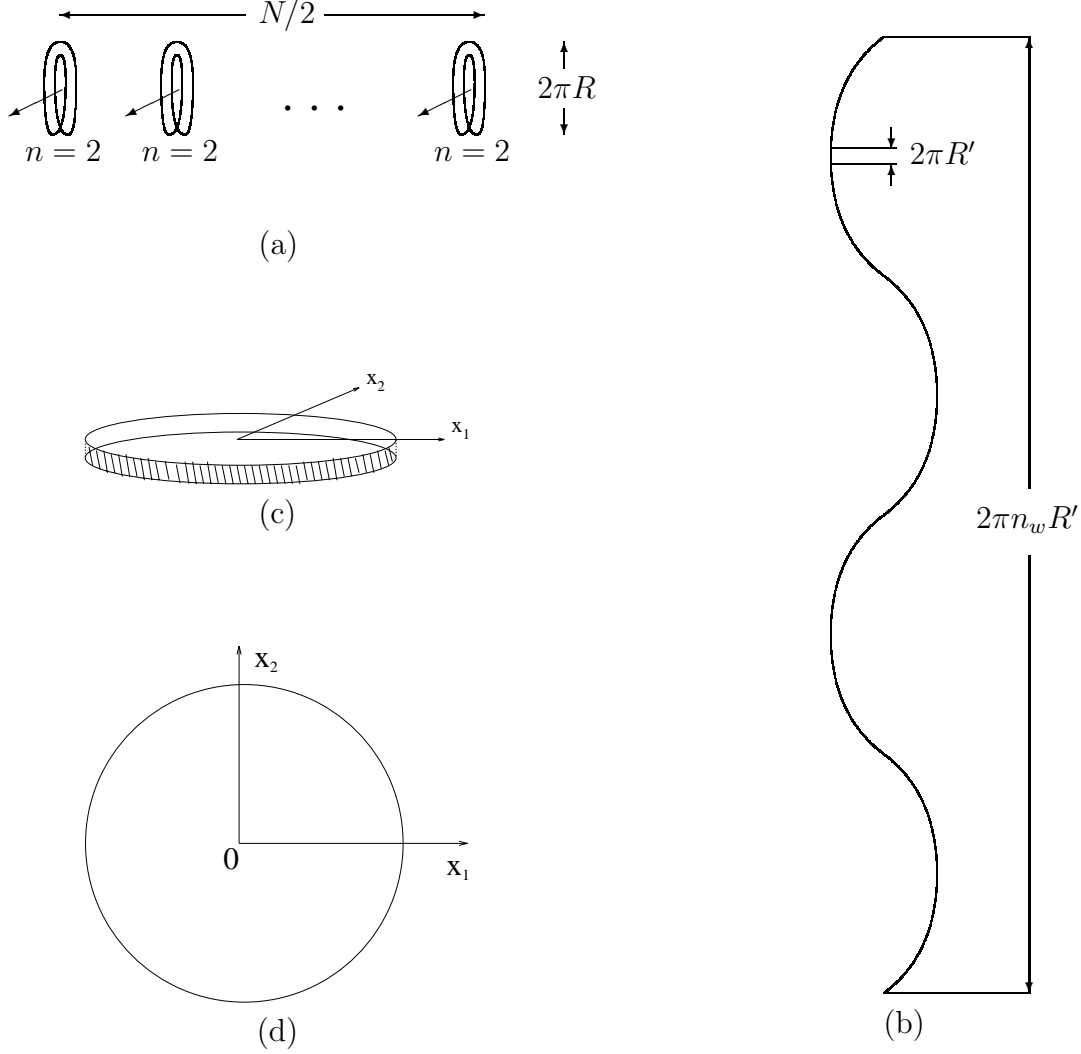


Figure 4: (a) Component strings for the D1-D5 microstate  $[\sigma_2^{--}]^{N/2}$ . (b) The fundamental string in the dual FP system, oscillating in the harmonic  $n = 2$ , shown opened up to its full length  $2\pi n_w R'$ . (c) The string of (b) as it actually appears due to the identification  $y' \rightarrow y' + 2\pi R'$ . (d) The cross section of the singularity created by the strands in (c) in the classical limit.

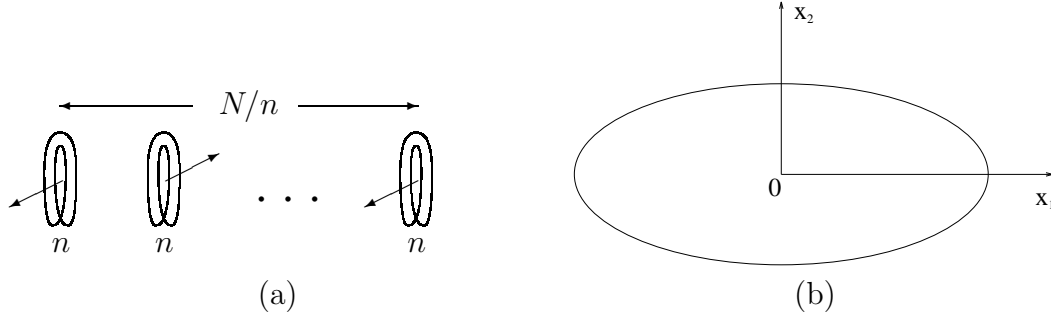


Figure 5: (a) Component strings with spins *not* all aligned; (b) The shape of the singularity.

Mapping by dualities back to the D1-D5 system we get the metrics (2.10) with  $j_L = j_R = \frac{N}{2n}$ . If we take  $n = 1$  then we get the maximal possible angular momentum  $(j_L, j_R) = (\frac{N}{2}, \frac{N}{2})$ ; it was shown in [16] that the corresponding D1-D5 supergravity solution was a smooth geometry.

(ii) The states described in (i) correspond, in the list (2.9), to  $j$  taking its maximal possible value  $\frac{N}{2n}$ . If all the  $\frac{N}{n}$  spins are not aligned, then from the same set of ‘component strings’ we can get smaller values of  $j$ . In the dual FP system these latter states are just obtained by taking the same harmonic on the fundamental string, but making the string swing around an ellipse rather than a circle:

$$x'_1 = A \cos\left(\frac{n}{R'n_w}(y' + t')\right), \quad x'_2 = B \sin\left(\frac{n}{R'n_w}(y' + t')\right) \quad (4.12)$$

The string still forms a helix but covers a surface with elliptical cross section as depicted in figure 5. In particular letting the string vibrate only in one direction (e.g.  $B = 0$  in (4.12)) would give  $j_L = j_R = 0$ . The supergravity solution for this case is written down explicitly in Appendix I.

(iii) Consider a chiral primary that has twist operators of two different orders, for example

$$[\sigma_n^{--}]^{m_1} [\sigma_{2n}^{--}]^{m_2}, \quad nm_1 + 2nm_2 = N \quad (4.13)$$

In the FP dual we have harmonics of order  $n$  and  $2n$  on the string, so the waveform looks like

$$\begin{aligned} x'_1 &= A_1 \cos\left(\frac{n}{R'n_w}(y' + t')\right) + A_2 \cos\left(2\frac{n}{R'n_w}(y' + t')\right), \\ x'_2 &= B_1 \sin\left(\frac{n}{R'n_w}(y' + t')\right) + B_2 \sin\left(2\frac{n}{R'n_w}(y' + t')\right) \end{aligned} \quad (4.14)$$

The surface covered by the string now has a more complicated cross section, depicted in figure 6. For a range of parameters  $A_i, B_i$  the singularity curve exhibits a self intersection.

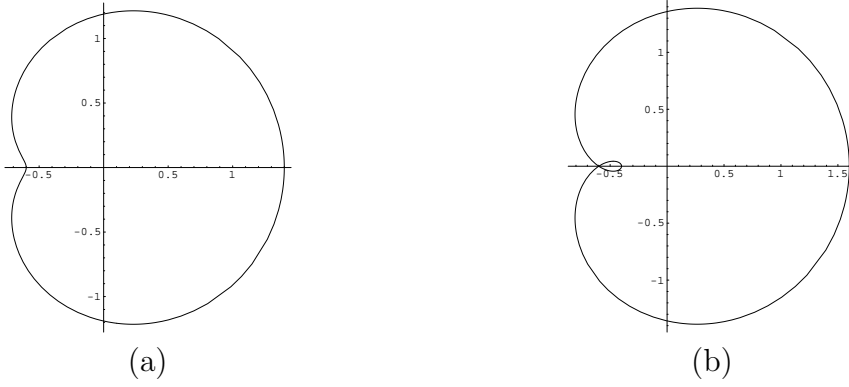


Figure 6: The singular curve when the FP string carries two different harmonics: eqn. (4.14) parameter values (a)  $A = 1, B = 0.4$ ; (b)  $A = 1, B = 0.6$ .

Such self-intersections are not generically present however, since the singular curve lies in a 4-dimensional space  $\vec{x}'$ .

(iv) More generally, the singularity can have the shape of a general curve. Let the string in the FP solution be described by the profile  $\vec{x}' = \vec{G}(v)$ . (Here  $\vec{x}'$  is a 4 component vector  $\{x'_1, x'_2, x'_3, x'_4\}$ .) For a generic state the typical wavelength involved in the oscillations is much larger than the compactification radius  $R'$  of the  $y'$  coordinate. Then for any fixed  $y' = y'_0$  the string passes through a set of points  $\vec{x}'$  that are closely spaced along a smooth curve. This curve is given parametrically by

$$\vec{x}' = \vec{G}(\alpha), \quad 0 \leq \alpha < 2\pi n_w R'. \quad (4.15)$$

(By construction this curve is independent of the choice of  $y'_0$ .) In the classical limit the spacing of points along the curve goes to zero. Thus the classical geometry that corresponds to this microscopic FP solution has a singularity along the curve  $\vec{x}' = \vec{G}(\alpha)$ , with the singularity extending over all  $0 \leq y' < 2\pi R'$  and for all  $t$ . We will not explicitly mention in what follows the extent in the  $y', t$  directions, and characterize the singularity by the shape of the singular curve (4.15).

It is important that in the classical limit the large value of the winding  $n_w$  gives a singularity structure that is invariant under translations in  $y'$ . This invariance in  $y'$  allows us to apply T-duality along  $y'$ , which is needed to obtain the corresponding D1-D5 solution. The latter solution will also have a singularity that is a curve in the space  $\vec{x}$ , and which extends uniformly in the  $y, t$  directions. The singular curve for the D1-D5 geometry is

$$\vec{x} = \vec{F}(\alpha), \quad \vec{F} = \frac{g}{R\sqrt{V}} \vec{G} \quad (4.16)$$

Given that the curve (4.16) is a 1-D subspace in 4 dimensions, the following situation is generic:

- (i)  $\vec{x} = \vec{F}(\alpha)$  is a simple closed curve with no self-intersections.

- (ii)  $|\dot{\vec{F}}(\alpha)| \neq 0$  at all points along the curve.

Note that in the FP system if we take any  $y' = y'_0$  and look for the points in the  $\vec{x}'$  space through which the string passes, then the number of these points per unit length along the curve (4.15) is

$$|\dot{\vec{G}}(\alpha)|^{-1} \frac{1}{2\pi R'} \quad (4.17)$$

The singularity is characterized by both its shape and the ‘density’ (4.17).

Let us look at the D1-D5 system and examine the geometry for a general singular curve  $\vec{F}$ . By translational invariance we can set

$$\int_0^L dv F_i(v) = 0. \quad (4.18)$$

We will also assume that singularity is confined in the region with a typical size  $a$ , which means that

$$F_i(v) F_i(v) \leq a^2 \quad \text{for all } v \quad (4.19)$$

The throat geometry then has the following two properties:

- (i) For  $\vec{x}^2 \gg a^2$  we get the metric (Appendix E)

$$ds^2 \approx -\frac{1}{h}(dt^2 - dy^2) + h d\vec{x} d\vec{x}, \quad (4.20)$$

where

$$h = \left[ \left( 1 + \frac{Q_5}{\vec{x}^2} \right) \left( 1 + \frac{Q_1}{\vec{x}^2} \right) \right]^{1/2} \quad (4.21)$$

If we compute the time of flight for a quantum from the start of the throat to  $r = a$  and back then we get

$$\Delta t_{SUGRA} = \pi \frac{\sqrt{Q_1 Q_5}}{a} \quad (4.22)$$

(ii) The geometry ends smoothly at  $r \sim a$  except for the singular curve. We show in Appendix F that waves incident on the singular curve in fact reflect from the curve, as long as we have the genericity conditions (i) and (ii) mentioned above for the curve. In Appendix G we estimate the maximum time  $\Delta t_{sing}$  that a quantum can spend in the vicinity of the singularity even if it heads radially into the singularity from  $r \sim a$ . We find that

$$\Delta t_{sing} \sim \frac{2}{\pi \sqrt{\bar{n}}} \Delta t_{SUGRA} \quad (4.23)$$

where  $\bar{n}$  is the average winding number of the component strings, and so  $\bar{n} \geq 1$ .<sup>3</sup>

---

<sup>3</sup>Note that for the metrics (2.10) we have performed the exact computation for the travel time  $\Delta t_{SUGRA}$  (eq. (3.7)); this time includes all effects of approaching the singularity and returning back, so that we do not need to consider separately the time  $\Delta t_{sing}$  spent near the singularity.



Putting together properties (i) and (ii) we find that

$$\Delta t_{CFT} \sim \Delta t_{SUGRA} \quad (4.24)$$

We in fact expect an exact match between the CFT and supergravity, but if all the component strings in the CFT are not of equal length then  $\Delta t_{CFT}$  can only be defined upto some spread. Similarly the waveform in the supergravity throat returns with some distortion and thus  $\Delta t_{SUGRA}$  has a spread as well. For this reason the above relation appears as an approximate one, but in the cases where these time scales could be exactly defined and computed we obtained the exact equality (3.13).

### 4.3 ‘Hair’ in the D1-D5 geometry.

For geometries that have a black hole horizon there exists the well known ‘no hair’ conjecture, which states that the microstates of the hole will not be visible in its geometry. While this conjecture may indeed not be valid as a general theorem, it is nevertheless true that we do not know how to see the entropy of black holes as a count of different spacetime geometries. Thus for the D1-D5 momentum black hole in 4+1 dimensions, the metric lifted to 6-D is

$$ds_E^2 = -\frac{1}{h}(dt^2 - dy^2) + \frac{Q_P}{hr^2}(dt + dy)^2 + h \left[ dr^2 + r^2 d\Omega_3^2 \right]. \quad (4.25)$$

Classically this metric represents all the  $\sim e^{2\pi\sqrt{n_1 n_5 n_p}}$  microstates of the hole. If we set the momentum charge to zero, we still find  $\sim e^{2\sqrt{2}\pi\sqrt{n_1 n_5}}$  microstates. The geometry (4.25) reduces to

$$ds_E^2 = -\frac{1}{h}(dt^2 - dy^2) + h \left[ dr^2 + r^2 d\Omega_3^2 \right]. \quad (4.26)$$

The classical horizon area is now zero, but the classical geometry (4.26) still seems to exhibit a version of ‘no hair’, since it is the same for all microstates. How do we reconcile this situation with the fact that we have found different throat geometries for different microstates of the D1-D5 system?

It turns out that the geometry produced by generic microstates all behave as (4.26) upto a ‘classical’ distance down the throat (so that we see no hair) (figure 7a), but start to differ at a distance which is  $\sim 1/\hbar$  down the throat, where we find the the end of the throat and the above discussed singularities (figure 7b). More precisely assume fixed the parameters of the string background, and take the limit  $n_1, n_5 \rightarrow \infty$  – this is the classical limit of the solutions. The radius of the throat is  $(Q_1 Q_5)^{\frac{1}{4}} \sim (n_1 n_5)^{\frac{1}{4}}$ . Choose any dimensionless number  $\mu$ , and look at distances that are reached by a particle falling down the throat for a time  $t \sim \mu(Q_1 Q_5)^{\frac{1}{4}}$ . As  $n_1, n_5 \rightarrow \infty$ , the metrics for generic microstates will all become the same in this domain in the throat. The end of the throat comes for  $t \sim (n_1 n_5)^{1/2}$ , and in the classical limit this will appear to be infinitely far

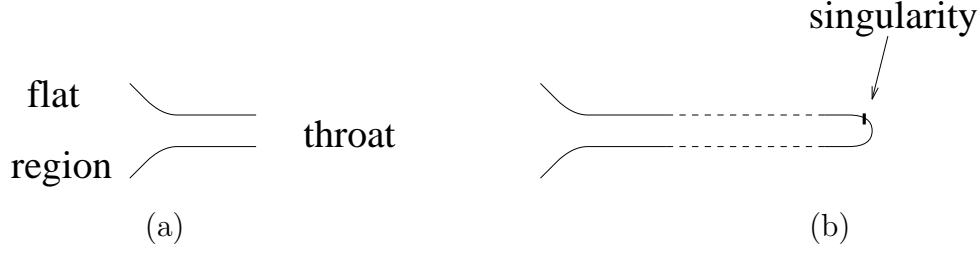


Figure 7: (a) A leading order classical analysis suggests an infinite throat; (b) The throat actually ends at a distance that diverges as  $\hbar \rightarrow 0$ .

down the throat. Thus we recover a ‘no hair’ classical limit, but see different geometries for different microstates near the end of the throat.

#### 4.4 A flat space computation to understand the size of the singularity

An essential part of the above results can be understood by considering the string of the FP system in flat space. It was crucial in obtaining  $\Delta t_{CFT} \sim \Delta t_{SUGRA}$  that the size of the singularity, for fixed winding and momentum charges, depended on the *wavelength* of the oscillations and not on the angular momentum they carried. Let the F string have total length  $L_T = 2\pi n_w R'$ . Let it carry  $n_p$  units of momentum which implies the energy of vibration

$$E = \frac{n_p}{R'} \quad (4.27)$$

Further, let the wavelength of the vibrations be  $\lambda \sim L_T/n$ . The Hamiltonian for small vibrations is

$$H = \frac{T}{2} \int_{z=0}^{z=L_T} dz \left[ \left( \frac{d\vec{x}'}{dt} \right)^2 + \left( \frac{d\vec{x}'}{dz} \right)^2 \right] \quad (4.28)$$

By the virial theorem

$$\langle H \rangle = T \left\langle \left( \frac{d\vec{x}'}{dz} \right)^2 \right\rangle L_T \sim T \langle x'^2 \rangle \frac{2\pi}{n_w R'} n^2 \quad (4.29)$$

Setting  $\langle H \rangle = E$  we get

$$\langle x'^2 \rangle^{1/2} \sim \left( \frac{N}{2\pi T} \right)^{1/2} \frac{1}{n} \quad (4.30)$$

Thus we see that (for fixed  $N$ ) the rough size of the singularity depends on  $n$ , which determines the wavelength in the FP solution, and maps to the winding number of individual component strings in the dual D1-D5 system. In the supergravity solution the size of the singularity determines the approximate end of the throat, and we see from the above analysis that for the D1-D5 system the effective length of the throat is determined by the number of component strings rather than the angular momentum of the configuration.

For large  $N$ , the generic ground state of the FP system has  $\sim \sqrt{N}$  quanta of vibration modes with wavelength  $\sim L_T/\sqrt{N}$ . In the dual D1-D5 system we find that for the geometries (2.10) we have  $\gamma \sim 1/\sqrt{N}$ , which is zero in the classical limit.

In Appendix H we compute the length of the singular curve for the D1-D5 bound state in flat space. Multiplying this length with the height  $2\pi R$  of the singularity in the  $y$  direction we find for the area of this classical singularity

$$Area \leq 4\pi\sqrt{2}\sqrt{NG^{(6)}} \quad (4.31)$$

where equality is attained only for the cases where all component strings have the same length.

## 4.5 Nonsymmetric excitations of component strings

Let the CFT state have  $m$  component strings. Note that the calculation of Appendix A for the amplitude of absorption/emission from the component string did not depend on the length of the component string. Thus an incident graviton will create an excited state of the form

$$|\psi\rangle_{excited} = \frac{1}{\sqrt{m}}[(string\ 1\ excited) + (string\ 2\ excited) + \dots + (string\ m\ excited)] \quad (4.32)$$

If all the  $m$  component strings were identical, then (4.32) is the only state allowed by Bose symmetry; this is the state that we used in the computation of Appendix A. But in general the  $m$  component strings will not be in the same state – they may have different lengths or different spin orientations. Then instead of (4.32) we can get the more general state

$$|\psi\rangle_{excited} = \alpha_1(string\ 1\ excited) + \alpha_2(string\ 2\ excited) + \dots + \alpha_m(string\ m\ excited) \quad (4.33)$$

As a simple example, take the R ground state  $[\sigma_{N/m}^{--}]^{m/2}[\sigma_{N/m}^{++}]^{m/2}$  and consider it excited to the nonsymmetrical combination

$$|\psi\rangle_{excited} = \frac{1}{\sqrt{2}}[(\sigma^{--}\ string\ excited) - (\sigma^{++}\ string\ excited)] \quad (4.34)$$

A naive calculation would now suggest that the amplitude to emit a graviton from this state is zero – the amplitude for emission from the two parts of the state give a total amplitude  $\frac{1}{\sqrt{2}}[R - R] = 0$  ( $R$  is the amplitude of emission from either type of component string). It would thus seem that there are CFT excitations that are decoupled from the supergravity modes at infinity.

But a closer look reveals that this naive computation requires the following modification. We have seen above that the singularity of the D1-D5 system is not a point in the space  $\vec{x}$  but rather an extended curve. Even in the limit of weak coupling when we have

the ‘branes in flat space’, the location of the branes will be along this curve of nonzero extent (see Appendix H for a computation of the length of the singular curve). In the emission calculation if the component strings were all at one point then the graviton emission amplitude would indeed vanish for the state (4.34). But the finite extent of the singularity implies that even if the leading order s-wave emission is cancelled by a judicious choice of phase as in (4.34), the excitation will decay (though more slowly) through the emission of p wave and higher partial wave gravitons.

We can see the presence of states analogous to (4.33) in the dual supergravity. A simpler example can be found using an unbound state rather than a single bound state. Thus consider two identical D1-D5 bound states, each corresponding to the CFT state  $\sigma_N^{--}$ . Construct a superposed state where the centers of the two components are placed a distance  $b$  apart, with  $b \ll (Q_1 Q_5)^{1/4}$ . Then the supergravity solution exhibits a single ‘combined’ throat for a certain distance, and then the throat branches into two smaller throats, which we call throat 1 and throat 2.<sup>4</sup>

An s-wave scalar traveling down the combined throat enters throat 1 and throat 2 with equal amplitude. But we can also construct a wavefunction for the scalar which has *opposite* amplitudes in throat 1 and throat 2. How will such a wavefunction emerge into the combined throat and thus out to infinity?

While the above wavefunction does not emerge into the combined throat as an s-wave, it does have a nonzero amplitude to emerge as a p-wave. The p-wave has a smaller amplitude to exit the combined throat, and thus we see a suppression in the radiation rate for such a wavefunction.

In a general state of the D1-D5 system the end of the throat exhibits no particular symmetry, and so an s-wave going down the throat can get converted to a mixture of harmonics after reflection from the end of the throat. The geometries (2.10) are special however, since the different harmonics separate exactly and an s-wave returns as an s-wave. The corresponding CFT states are special too, since their excitation takes the symmetrical form (4.32) and not the more general form (4.33).

## 5 Breakdown of the semiclassical approximation and the threshold of formation of black holes

### 5.1 Several vibration modes on the same component string

Consider an s-wave minimally coupled scalar, with energy  $\omega$ , traveling up and down the throat of the D1-D5 geometry. We have seen that this maps in the CFT to a left moving and a right moving vibration mode on the effective string, each with energy  $\omega/2$ . In particular we had noted (eqn. (3.2)) the maps

$$h_{67} \rightarrow \frac{1}{\sqrt{2}} (|x_6\rangle_L \times |x_7\rangle_R + |x_7\rangle_L \times |x_6\rangle_R)$$

---

<sup>4</sup>Branching throats were considered in a slightly different context in [36].

$$B_{67}^{RR} \rightarrow \frac{1}{\sqrt{2}} (|x_6\rangle_L \times |x_7\rangle_R - |x_7\rangle_L \times |x_6\rangle_R) \quad (5.1)$$

We will find it convenient to work with the linear combinations

$$\begin{aligned} S_{67}^+ &\equiv \frac{1}{\sqrt{2}}[h_{67} + B_{67}^{RR}] \rightarrow |x_6\rangle_L \times |x_7\rangle_R \\ S_{67}^- &\equiv \frac{1}{\sqrt{2}}[h_{67} - B_{67}^{RR}] \rightarrow |x_7\rangle_L \times |x_6\rangle_R \end{aligned}$$

### 5.1.1 Throat corresponding to the CFT state with one component string.

Consider the R ground state that arises from the chiral primary  $\sigma_N^{--}$ . This state has one ‘component string’ wound  $n_1 n_5$  times around the circle of radius  $R$  (figure 1a), and thus has the longest possible throat ( $\Delta t_{CFT} = \Delta t_{SUGRA} = \pi n_1 n_5 R$ ). Place in this throat a quantum of  $S_{67}^+$  with energy

$$\omega = \frac{2}{n_1 n_5 R} \equiv \omega_0 \quad (5.2)$$

This gives left and right vibrations on the effective string of energy  $1/n_1 n_5 R$  each, which is the lowest energy excitation possible.

Now imagine that we *also* place in the throat a quantum of  $S_{89}^+$  with energy  $\omega_0$ . In the CFT we get the state

$$S_{67}^+(\omega_0) S_{89}^+(\omega_0) \rightarrow |x_6\rangle_L |x_8\rangle_L \times |x_7\rangle_R |x_9\rangle_R \quad (5.3)$$

But now look at the CFT state corresponding to the supergravity scalars  $S_{69}^+(\omega_0), S_{78}^+(\omega_0)$ :

$$S_{69}^+(\omega_0) S_{78}^+(\omega_0) \rightarrow |x_6\rangle_L |x_8\rangle_L \times |x_7\rangle_R |x_9\rangle_R \quad (5.4)$$

The supergravity states in (5.3), (5.4) are different (the scalars involved are not the same in the two cases) but they seem to map to the same state in the CFT. It would appear that we have found a contradiction with the proposed duality map.

But note that these quanta in the throat have an energy of order  $\sim 1/n_1 n_5 R$  or greater. It was shown in [12] that for this throat geometry the threshold of horizon formation is

$$\Delta E_{threshold} \sim \frac{1}{n_1 n_5 R} \quad (5.5)$$

*Thus just when we seemed to be getting a contradiction between the CFT effective string and the throat geometry, we find that the physics changes because of black hole formation.*

Note that for this particular state of the CFT the supergravity approximation will not be good even to describe the propagation of one quantum to the end of the throat, since the backreaction on the geometry will deform the geometry by order unity.

### 5.1.2 Throats corresponding to CFT states with $m$ component strings.

Let us see how the above discussion extends to states of the CFT that have  $m > 1$  component strings. Let the CFT state be composed of  $m$  component strings with winding number  $\sim N/m$  each. Then in the supergravity solution we see that (eq. (2.15))

$$a \sim \frac{m}{n_1 n_5} \sqrt{Q_1 Q_5} \frac{1}{R} \quad (5.6)$$

The throat ends at  $r \sim a$  while for  $r \gg a$  it has the geometry (4.26) of the D1-D5 system with no rotation. In the geometry (4.26) if we add a nonextremal energy  $\Delta E$  then we get a horizon at

$$r_H = \left[ \frac{2g^2 \Delta E}{RV} \right]^{\frac{1}{2}} \quad (5.7)$$

(we have set  $\alpha' = 1$ ). Thus  $r_H \gg a$  then we get horizon formation, while if  $r_H \ll a$  then the matter quanta just move back and forth in the throat, giving the ‘hot tube’ [12]. The threshold energy for black hole formation  $\Delta E_{threshold}$  is then obtained by setting  $r_H \sim a$ , which we write in a suggestive fashion as

$$\Delta E_{threshold} \sim \frac{m^2}{n_1 n_5 R} = m \left( \frac{1}{\frac{N}{m} R} \right) \quad (5.8)$$

*We see that a black hole forms if we have enough energy to excite one quantum of the lowest allowed vibration mode on each component string.*

The minimum wavelength that fits in the throat is  $(m\omega_0)^{-1}$ . Note that we can place  $1 \ll m_1 \ll m$  quanta of this wavelength in the throat without any significant deformation of the throat geometry. Thus supergravity analysis performed in subsection 3.3 using the test particle approximation is seen to be valid, as long as we do not take too high an energy ( $E > m^2 \omega_0$ ) for this test particle.

To summarize, we have seen that if we place more than one pair of vibration modes on each component string, then the naive count of supergravity states fails to agree with the count in the CFT (eqs. (5.3, 5.4)). But the energy required to excite the lowest vibration on each component string turns out to equal  $\Delta E_{threshold}$ , the energy to form a black hole; thus the physics changes at this point, and a contradiction is averted.<sup>5</sup>

## 5.2 Black hole formation

Thus far we have ignored all interactions when dealing with the ‘component strings’ in the CFT; we just considered left and right moving vibration modes on individual component strings. But the supergravity solution does not in general map to the CFT at the orbifold

---

<sup>5</sup>In [37] it was found that in the  $c = 1$  matrix model ( $D = 2$  string theory) the process of ‘fold formation’ distributed an initial energy  $m^2$  as  $\sim 1 + 2 + \dots + m$ ; i.e. we get one quantum each of frequencies  $1, 2, \dots, m$ . It may be that the interactions in the present problem distribute energies in this fashion rather than  $m^2 \sim m + m + \dots + m$  as was suggested by (5.10).

point  $M^N/S_N$ ; we have a deformation of the orbifold by blowup modes [21, 24]. Such deformations can be generated by  $(1, 1)$  operators of the form  $\psi\bar{\psi}\sigma_2$ : the chiral primary  $\sigma_2$  has dimensions  $(\frac{1}{2}, \frac{1}{2})$  and  $\psi, \bar{\psi}$  are dimension  $\frac{1}{2}$  fermions from the left and right sectors. This operator cuts or joins component strings, at the same time creating a left and a right moving fermionic excitation on the resulting component strings [33].

To see what this interaction might do, let us look at the location of the horizon  $r_H$  (eqn. (5.7)) when we throw in an energy  $\Delta E \gg \Delta E_{threshold}$ . (We still assume that  $\Delta E$  is low enough that the horizon forms in the throat rather than outside.) From our map between the supergravity throat and the CFT we find that when a quantum travels from the start of the throat to  $r = r_H$  then on the CFT string the two vibration quanta separate by a distance equal to the time of flight to  $r_H$ :

$$l_H = (Q_1 Q_5)^{1/2} \int_{r_H}^{(Q_1 Q_5)^{1/4}} \frac{dr}{r^2} \sim \frac{(Q_1 Q_5)^{1/2}}{r_H} \quad (5.9)$$

This requires the CFT string to have length at least  $2l_H$ . When a black hole forms we must clearly expect some change in the description on the CFT side. Using (5.7) we find that

$$\Delta E \sim \frac{4\pi}{2l_H} \left( \frac{2\pi n_1 n_5 R}{2l_H} \right) \quad (5.10)$$

*Thus we see that if the interaction were to change the CFT state to one where all the component strings had length  $2l_H$ , then the energy  $\Delta E$  would excite the lowest allowed vibration energy  $\frac{4\pi}{2l_H}$  on each of the resulting  $\frac{2\pi n_1 n_5 R}{2l_H}$  component strings.*

Even though we are not investigating the interaction in detail here, there are two features of the interaction that deserve comment. First, below the black hole formation threshold we have obtained good results by ignoring the interaction altogether.<sup>6</sup> Secondly, when a horizon does form (and thus interactions presumably become relevant) then we seem to need enough energy to excite *all* the component strings. We speculate now on how this ‘all or none’ feature of the interactions might arise.

In the CFT the normalized interaction operator has the form

$$\psi\bar{\psi}\sigma_2 \sim \frac{1}{N} \sum_{i,j=1}^N \psi\bar{\psi}\sigma_{ij} \quad (5.11)$$

Let us start with a CFT state which has  $n_1 n_5$  singly wound component strings, and let the first string carry a pair of vibrations. The above interaction can join another string to the first one, giving a state of the form

$$|\psi_f\rangle \sim \frac{1}{\sqrt{N-1}} [(12) + (13) + \dots (1N)] \quad (5.12)$$

---

<sup>6</sup>This may no longer be true when we have a bound state with component strings of different lengths. The shape of the singularity is obtained by mapping to the dual FP system where the F string carries harmonics of two different orders. The resulting singularity shape depends in a complicated way on all the harmonics present, so we expect some interaction effects between the component strings in the CFT.

From (5.11), (5.12) we see that the interaction generates a change

$$|\psi_f\rangle \sim \frac{1}{\sqrt{N}} |\psi_i\rangle \quad (5.13)$$

This small parameter  $\frac{1}{\sqrt{N}}$  is also the coupling constant of supergravity in  $AdS_3$ , so it appears that ignoring interactions in the CFT was equivalent to ignoring gravity corrections at leading order in the dual supergravity.

If we use several such interactions, then we get further suppression by powers of  $\frac{1}{\sqrt{N}}$ . But now suppose that we convert all the initial component strings to component strings of length 2, each carrying, say, the lowest vibration mode. Then because all these component strings will be in the same state, we get a ‘Bose enhancement factor’ – if there are already  $\sim N$  units of a given component string then creating the next one gives a factor  $\sim \sqrt{N}$ . Thus while the amplitude may be small to create a few interactions, it may be order unity if it affects almost all the component strings, which is what we observed in the process of horizon formation.<sup>7</sup>

### 5.3 Validity of the supergravity approximation

We have noted after eqn. (5.8) that if the number of component strings is  $m \gg 1$  then the backreaction of a quantum with energy  $E \ll m^2 \omega_0$  will not make a significant distortion to the geometry ( $m^2 \omega_0 = \Delta E_{threshold}$ , the threshold for black hole formation). The geometry of the throat is (except near the end) locally  $AdS_3 \times S^3 \times M$ ; since this is an exact string solution it is not modified by stringy corrections. As we go down the throat the sizes of  $S^3$  and  $M$  do not change, but the length of the  $y$  circle shrinks. One might wonder if this leads to a large effective coupling constant for quanta deep in the throat, thus possibly invalidating the linear wave equation we have used for the propagation of the scalar. But in [12] it was shown that if the scalar has for instance an interaction  $\phi^3$  then this interaction becomes relevant only after a distance down the throat corresponding to a time of flight  $\sim n_1 n_5 R$ . But the end of the throat is reached after the quantum travels for a time  $\sim n_1 n_5 R/m$ . Thus again we find that if  $m \gg 1$  the interactions can be ignored, and we can use the linear wave equation to explore the end of the throat at  $r \sim a$ .

## 6 A proposal to resolve the information paradox

In [18] it was argued that the information paradox is resolved if we assume that spatial slices in a foliation cannot be *stretched* too much. We review this argument, and then relate it to the computations of the present paper.

---

<sup>7</sup>The issue of a ‘phase transition’ at the threshold of black hole formation was discussed in [38].



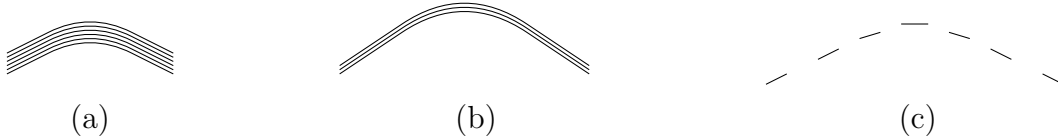


Figure 8: (a) An initial hypersurface with a high density of degrees of freedom; (b) Stretching dilutes these degrees; (c) The degrees of freedom are so sparse that usual local physics breaks down.

## 6.1 The argument.

The information paradox arises because we can find a smooth region in the black hole spacetime which can be given a ‘nice’ foliation by spacelike hypersurfaces; the spatial slices satisfy all the smoothness conditions that we might wish to impose. On the initial slice we have a regular distribution of matter, while late time slices capture both the initial matter and the corresponding outgoing Hawking radiation. (The slices do not approach the singularity.) Since information cannot be ‘duplicated’, we must somehow have ‘bleached’ the information out of the matter and transferred it to the radiation, in the course of the evolution. But before we can postulate the existence of some nonlocal process to accomplish this goal we must identify the ‘trigger’ for the process: what distinguishes the smooth foliation of this region of the black hole spacetime from the foliation of a smooth manifold without black holes? In the absence of such a ‘trigger’ criterion, the postulated nonlocal process would invalidate normal quantum evolution even in the absence of black holes.

Since the foliation is smooth, the trigger cannot involve short distance quantum gravity effects. Two features are however observed in the smooth black hole foliations. The first is that one part of the spacelike slice evolves much slower than the other. This is the ‘redshift effect’ familiar in black hole geometries. But if we consider a scalar field evolving along the foliation, we see no reason why this differential evolution should invalidate normal quantum evolution. String theory is more complicated, but here again there is no convincing reason why the differential evolution rates would lead to nonlocal information transport (see however [39]). These are the standard difficulties that one runs into when trying to resolve the information problem.

The second feature of the slices is that they *stretch* exponentially in the course of the evolution. More precisely, if we want the slices to be smooth (thus they should not go near the singularity) then the price that we must pay is that a region of the initial slice (with radius  $\sim R_s$ , the Schwarzschild radius) will get ‘stretched’ to a final length that is  $\sim O(1/\hbar)$  and thus nonclassical.

It was argued in [18] that spatial slices should be attributed a ‘density of degrees of freedom’. Stretching dilutes these degrees. If we place more matter quanta in a region of the slice than there are available degrees of freedom then semiclassical evolution breaks down and nonlocal information transport can be triggered (Figure 8). This new way of violating the semiclassical approximation allows information leakage in Hawking radiation

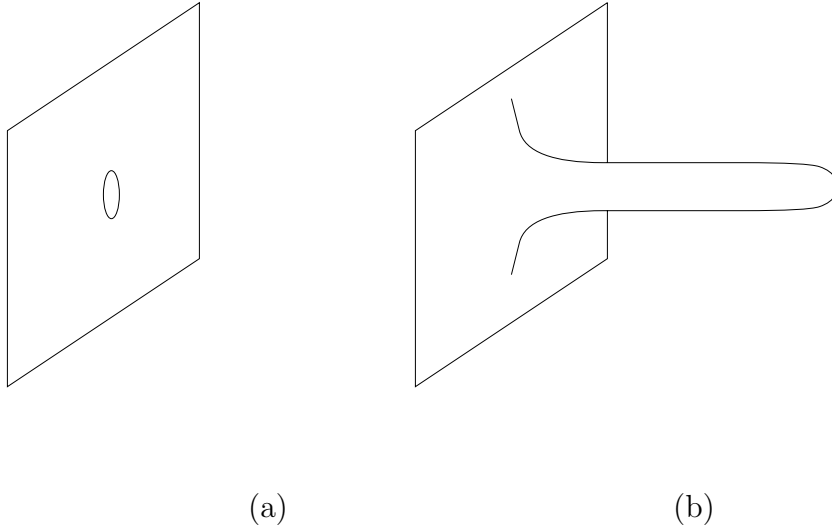


Figure 9: (a) Flat spacetime in the absence of the branes; (b) The presence of branes stretches the region marked in (a) to a long throat.

while preserving locality of quantum mechanics in the absence of black holes, and thus the information paradox would be resolved. The length of this critically stretched slice was expressed in [18] in terms of the number of degrees of freedom  $e^S$  ( $S$  is the black hole entropy), but noting that the separation of these degrees along the slice was order the Schwarzschild radius  $R_s$ , we can write the critically stretched length of the slice as

$$s_{max} \sim \frac{\mathcal{V}}{G_N} \quad (6.1)$$

where  $\mathcal{V}$  is the volume enclosed in *flat* space in a ball of radius  $\sim R_s$ .

The above arguments can be made on very general grounds, reflecting the universal nature of the information problem. Let us now see what aspects of this picture emerge in our D1-D5 system.

## 6.2 ‘Stretching’ of slices in the D1-D5 system

(i) In the absence of the D1, D5 branes the spacetime geometry is flat (figure 9a). The branes deform the geometry to a long but finite throat. Let us characterize the ‘stretching’ of the geometry by the time delay  $\Delta t_{SUGRA}$  caused by propagation down and back up the throat. We have found that the maximum value of this time delay is

$$\Delta t_{max} = \pi R n_1 n_5 \quad (6.2)$$

We wish to relate this length scale (6.2) to the size of the region *before* stretching. The radius  $\hat{r}$  of the ball drawn in figure 9b is  $\sim (Q_1 Q_5)^{1/4}$ . The radius of the  $S^3$  stabilizes

to a constant value in the throat (until we near the end), and for concreteness we set  $\hat{r}$  to this radius

$$\hat{r} = (Q_1 Q_5)^{1/4} \quad (6.3)$$

For this value of  $\hat{r}$  the enclosed volume in *flat* space (i.e. the space before deformation) is

$$\mathcal{V} = \frac{\pi^2}{2} (\hat{r})^4 = \frac{\pi^2}{2} Q_1 Q_5 \quad (6.4)$$

We now note that

$$\Delta t_{max} = \frac{\mathcal{V}}{2G_N^{(5)}} \quad (6.5)$$

where  $G_N^{(5)} = \frac{G_N^{(10)}}{(2\pi)^5 V R}$  and  $G_N^{(10)} = 8\pi^6 g^2 \alpha'^4$ . We observe that the relation (6.5) has the same form as (6.1).

It is noteworthy that the individual quantities in (6.5) depend on  $g, \alpha', V, R, n_1, n_5$  but these parameters appear only in certain physically intuitive combinations in the final relation. This fact leads one to believe that the relation (6.5) has a validity beyond the specific D1-D5 system being studied here.

(ii) Let the state in the D1-D5 CFT be given by  $\sim m$  component strings of winding number  $\sim N/m$  each. The time delay in the supergravity throat is then  $\Delta t_{SUGRA} \sim \Delta t_{max}/m$ . We have seen in section 5 that if more than  $\sim m$  supergravity quanta are placed in this throat geometry then we get evolution that departs from naive semiclassical expectations. *This suggests that a throat stretched to have a time delay  $\Delta t_{max}/m$  has just enough degrees of freedom to support  $\sim m$  quanta while maintaining the supergravity approximation.* This indicates a ‘dilution’ of the degrees of freedom when the throat is ‘stretched’ to longer lengths.

(iii) The argument of [18] requires that if we try to put more data on a slice than there are degrees of freedom then we will trigger nonlocal effects. Let us examine a similar feature that we find in our present study. Let the supergravity throat contain the two quanta  $S_{67}^+, S_{89}^+$ . Instead of putting these quanta in the lowest energy states in the throat let them have reasonably localized positions  $r_1 \neq r_2$ . Let the CFT state have only a few component strings. Then from the form of the wavefunctions (4.32) we see that there is a significant amplitude to have both pairs of vibrations on the same component string. But this CFT state can be regarded, as seen above in section 5, as describing with some amplitude the supergravity quantum  $S_{69}^+$ . If we try to extract the wavefunction for  $S_{69}^+$  however, we find that this supergravity quantum is not localized near either  $x_1$  or  $x_2$ .

To summarize, while we have not analyzed in the present paper the same spatial slices as those considered in [18], we have seen analogous phenomena of ‘stretching’ and consequent ‘dilution’ of degrees of freedom; further, the relations expressing the maximum stretch of spacelike slices (6.1), (6.5) appear to be similar.

## 7 Discussion

Let us summarize our results and note their relation to earlier work.

In [8, 13] the Poincare patch arising from the near horizon geometry was considered. It was noted that geometry stopped being *AdS* at large  $r$  ( $r > (Q_1 Q_5)^{1/4}$ ). The naive geometry eqn. (4.26) for the D1-D5 system (without rotation) extends as a uniform throat all the way down to a horizon at  $r = 0$ . What we have noted is that the throat ends at a certain point, and the location and nature of this end of the throat mirrors the D1-D5 microstate of the dual CFT. In the process we found that the metrics of [16] were only a small family out of a general family of metrics for the D1-D5 system, and we studied these more general metrics using chiral null models.

Having this end to the throat was crucial to all our considerations – if we took instead the naive geometry (4.26) then all quanta falling down the throat would reach the horizon at  $r = 0$  and create a black hole in the process. The actual ending of the throat implies a minimum threshold  $\Delta E_{threshold}$  for black hole formation, and yielded an energy domain below this threshold where we could set up a detailed duality map to the CFT. The finite length of the throat is essential to obtaining the relation  $\Delta t_{CFT} = \Delta t_{SUGRA}$ . In the analysis of [41] a quantum falling down the throat of the 3-brane geometry was represented by a spreading wavepacket in the CFT, but there was no analogue of the relation (3.13) since the infalling quantum did not turn back without horizon formation.

The finite length of the throat arises both from the truncation at small  $r$  ( $r \sim a$ ) and at large  $r$  ( $r \sim (Q_1 Q_5)^{1/4}$ ). We used explicitly the geometry at  $r \sim (Q_1 Q_5)^{1/4}$  (where the throat joins flat spacetime) in computing the radiation rate  $\mathcal{R}_{SUGRA}$  from the throat, and found that this equaled the radiation rate  $\mathcal{R}_{CFT}$  from the CFT state. Note that our computations were somewhat different from earlier studies [44] where the join of the AdS region to flat space was made at an arbitrary location in the AdS; the operator breaking conformal symmetry in the CFT then depended on this location.

It is remarkable that the black hole threshold for different microstates depends only on the energy scale  $1/R$  and the winding numbers of the component strings in the CFT. We noted that a breakdown of the semiclassical approximation occurred when there was more than one pair of vibration modes on the same component string. Such a proposal would appear to be closely related to the stringy exclusion principle, but there are some important differences which we now discuss.

The microscopic D1-D5 CFT is manifestly unitary and the degrees of freedom are limited. The information paradox asks for the implication of this fact in supergravity. It has often been argued that the ‘stringy exclusion principle’ [10] implies that there is a cut off in the order of spherical harmonics on the  $S^3$ . While this is probably true, it has not yielded any direct implications for the information problem, in part because the Hawking radiation is mostly confined to the first few spherical harmonics. What we have suggested here is that the cutoff of degrees of freedom in the CFT implies a maximal radial stretching of slices in the geometry, and the arguments of [18] then relate this to a resolution of the information paradox.

A further essential difference is that we are looking at non-BPS excitations, rather than the BPS quantities studied in [10, 20]. If we consider a component string wound  $n$  times on a circle of radius  $R$ , then left and right vibrations occur in fractional units but the total units of momentum must be an integer. Thus the lowest non-BPS excitation has energy  $\frac{2}{nR}$ , while the lowest BPS excitation has (for large  $n$ ) a much higher energy  $\frac{1}{R}$ . Correspondingly, we have found very low black hole thresholds for CFT states which have just one long component string. By contrast the black hole threshold discussed in [20] pertains to the NS sector of the CFT, and is a single, high energy threshold rather than a collection of thresholds depending on the particular CFT microstate.

Perhaps most interesting is the fact that we have found some support for the proposal of [18] that if we ‘stretch’ a spatial hypersurface too much then we will encounter a breakdown of normal semiclassical evolution, even though we would not see any of the usual factors that violate the semiclassical approximation like planckian curvature or planckian energies. It is interesting that the order of magnitude relation (6.1) emerging from [18] has the same form as the more precise relation (6.5), though we must note that the hypersurfaces involved in (6.1) and (6.5) are somewhat different. If the relation (6.5) turns out to be a general result, as we have conjectured, then we would find a profound change in our understanding of the ultimate structure of spacetime.

## Acknowledgments

We are grateful to T. Banks, I. Klebanov, F. Larsen and A. Strominger for useful discussions. This work was supported in part by DOE grant DE-FG02-91ER40690.

## A Rate of radiation from the effective string

Consider a string wrapped around the direction  $x_5 \equiv y$ . There is one right moving mode and one left moving mode on the string, with energy-momentum vectors given by (3.1). The polarizations of the vibration modes are given by the wavefunction (3.2). We wish to find the probability per unit time for these modes to interact and emerge from the string as a graviton.

The vertex that couples a left vibration mode, a right vibration mode, and a graviton is found by using the DBI action for the string [6, 7]. We first place the entire system in a large box. The volume of the noncompact directions  $x_1, x_2, x_3, x_4$  is  $V_{nc}$ , the volume of the compact  $T^4$  (in the directions  $x_6, x_7, x_8, x_9$ ) is  $(2\pi)^4 V$ , and the length of the  $x_5$  circle is  $2\pi R$ . Thus the volume of the 9-dimensional space is  $V_9 = (2\pi)^4 V (2\pi) R V_{nc}$ . We set  $\alpha' = 1$ . The 10-d Newton’s constant is  $G_N = 8\pi^6 g^2$ , and  $8\pi G_N = \kappa^2$ .

First consider the case where we have just one component string wrapped  $n_1 n_5$  times around  $y$ . For such a string in [7] we computed the amplitude per unit time for the state

$|6\rangle_L \times |7\rangle_R$  to decay into any given Fourier mode of the graviton  $h_{67}$ . This quantity is

$$\tilde{R}_h = \sqrt{2}\kappa|p_5| \frac{1}{\sqrt{2\omega}} \frac{1}{\sqrt{V_9}} \quad (\text{A.1})$$

where  $p_5$  is the momentum of any one of the vibration modes along  $x_5$ , and  $\omega$  is the energy of the graviton. For the state (3.1) of the vibration modes the amplitude per unit time will be higher by a factor  $\sqrt{2}$ . Using that  $|p_5| = \omega/2$  we get for the amplitude of decay per unit time

$$R_h = 2\kappa|p_5| \frac{1}{\sqrt{2\omega}} \frac{1}{\sqrt{V_9}} \quad (\text{A.2})$$

Using the ‘Fermi golden rule’ we find the probability of emission per unit time

$$\mathcal{R} = \frac{2\pi|R_h|^2}{\Delta E} \quad (\text{A.3})$$

where  $\Delta E$  is the spacing between levels for the graviton. The graviton has momentum only in the noncompact directions  $x_1, \dots, x_4$ . Thus

$$\Delta E = \frac{(2\pi)^4}{V_{nc}} \frac{1}{2\pi^2\omega^3} \quad (\text{A.4})$$

Putting all this together we finally get for the probability of emission per unit time

$$\mathcal{R} = \frac{\pi^2\omega^4 g^2}{2V(2\pi)R} \quad (\text{A.5})$$

Now consider the R ground state arising from the chiral primary  $[\sigma_{N/m}^{--}]^m$ . There are  $m$  component strings, each in the same state. Because of Bose symmetry between identical component strings, the wavefunction for the excited system must have the form

$$|\psi\rangle = \frac{1}{\sqrt{m}}[(\text{string 1 excited}) + (\text{string 2 excited}) + \dots (\text{string } m \text{ excited})] \quad (\text{A.6})$$

The amplitude  $R_h$  is now

$$R_h = \sqrt{m}2\kappa|p_5| \frac{1}{\sqrt{2\omega}} \frac{1}{\sqrt{V_9}} \quad (\text{A.7})$$

(there are  $m$  contributions each weighted by  $\frac{1}{\sqrt{m}}$ ). The probability per unit time for decay is then

$$\mathcal{R} = m \frac{\pi^2\omega^4 g^2}{2V(2\pi)R} \quad (\text{A.8})$$

## B Rotating D1–D5 system.

In this appendix we review some properties of the geometries (2.10). These metrics preserve a  $U(1) \times U(1)$  subgroup out of the  $SO(4)$  rotational symmetry of the  $S^3$ . As we have seen in this paper, these metrics represent only a small subclass of all the ground states of the D1–D5 system, but they are useful since the scalar wave equation factorizes in these backgrounds.

In supergravity approximation the system is parameterized by two charges  $Q_1$ ,  $Q_5$  and the rotation parameter  $a$ . The 10-D metric in the string frame is given by<sup>8</sup>:

$$\begin{aligned}
ds^2 = & -\frac{f_0}{\sqrt{f_1 f_5}}(dt^2 - dy^2) + \sqrt{f_1 f_5} \left( \frac{dr^2}{r^2 + a^2} + d\theta^2 \right) + \sqrt{\frac{f_1}{f_5}} \sum_{i=1}^4 dz^i dz^i \\
& + \frac{\sqrt{f_1 f_5}}{f_0} \left[ \left( r^2 + \frac{a^2 Q_1 Q_5 \cos^2 \theta}{f_1 f_5} \right) \cos^2 \theta d\psi^2 + \left( r^2 + a^2 - \frac{a^2 Q_1 Q_5 \sin^2 \theta}{f_1 f_5} \right) \sin^2 \theta d\phi^2 \right] \\
& - \frac{2Q_1 Q_5 a}{\sqrt{f_1 f_5}} \left[ \sin^2 \theta dt d\phi + \cos^2 \theta dy d\psi \right]
\end{aligned} \tag{B.1}$$

This system also has a nonzero value of dilaton field and the RR two-form  $C_{\nu\nu}^{(2)}$ :

$$\begin{aligned}
e^{2\Phi} &= \frac{f_1}{f_5}, & C_{ty}^{(2)} &= -\frac{2Q_1}{f_1}, & C_{t\psi}^{(2)} &= -\frac{\sqrt{Q_1 Q_5} a \cos^2 \theta}{f_1}, \\
C_{y\phi}^{(2)} &= -\frac{\sqrt{Q_1 Q_5} a \sin^2 \theta}{f_1}, & C_{\phi\psi}^{(2)} &= Q_5 \cos^2 \theta + \frac{Q_5 a^2 \sin^2 \theta \cos^2 \theta}{f_1}.
\end{aligned} \tag{B.2}$$

Here we have introduced three convenient functions:

$$f_0 = r^2 + a^2 \cos^2 \theta, \quad f_1 = f_0 + Q_1, \quad f_5 = f_0 + Q_5. \tag{B.3}$$

The coordinates  $z^1, \dots, z^4$  form a torus with volume  $(2\pi)^4 V$ , and  $y$  is compactified on a circle with circumference  $2\pi R$ .

From the microscopic point of view the system (B.1) describes a configuration of  $n_1$  D1 and  $n_5$  D5 branes with angular momentum  $J$ :

$$\begin{aligned}
n_1 &= \frac{V}{4\pi^2 g} \int_{S^3} e^{-\Phi} * H = \frac{Q_1 V}{g}, \\
n_5 &= \frac{1}{4\pi^2} \int_{S^3} H = \frac{Q_5}{g}, \\
j &= \frac{a V R}{2g^2} \sqrt{Q_1 Q_5}
\end{aligned} \tag{B.4}$$

Here  $g$  is the string coupling constant and we always put  $\alpha' = 1$ .

---

<sup>8</sup>In [34] we wrote the metric for rotating F1–NS5 system, but (B.1) can be obtained from it by applying the S duality transformation.

In appendix C we will also need the relation between the solution (B.1) and the solution for the rotating fundamental string carrying momentum. This relation was studied in detail in [34], here we just mention some facts which will later be used. Using the chain of string dualities one can map (B.1) into the solution describing the fundamental string which is wrapped  $n_5$  times around the  $y$  circle, it also carries  $n_1$  units of momentum and  $J$  units of angular momentum. The metric and matter fields of the solution describing the fundamental string can be written in terms of the chiral null model. To do this one should first go to the coordinates  $\tilde{r}, \tilde{\theta}$  instead of  $r, \theta$ :

$$\tilde{r} = \sqrt{r^2 + a^2 \sin^2 \theta}, \quad \cos \tilde{\theta} = \frac{r \cos \theta}{\sqrt{r^2 + a^2 \sin^2 \theta}}, \quad (\text{B.5})$$

and then introduce the Cartesian coordinates in the  $\tilde{r}, \tilde{\theta}, \phi, \psi$  space:

$$\begin{aligned} x_1 &= \tilde{r} \sin \tilde{\theta} \cos \phi, & x_2 &= \tilde{r} \sin \tilde{\theta} \sin \phi, \\ x_3 &= \tilde{r} \cos \tilde{\theta} \cos \psi, & x_4 &= \tilde{r} \cos \tilde{\theta} \sin \psi, \end{aligned} \quad (\text{B.6})$$

as well as two null coordinates:

$$u = t + y, \quad v = t - y. \quad (\text{B.7})$$

In the coordinates (B.6), (B.7) the geometry of the rotating string reads (see [34] for details):

$$\begin{aligned} ds^2 &= e^{2\Phi} \left( -du' dv' + \frac{Q'_1}{Q'_5} (e^{-2\Phi} - 1) dv'^2 - 4a' \sqrt{\frac{Q'_1}{Q'_5}} (e^{-2\Phi} - 1) \frac{x'_1 dx'_2 dv' - x'_2 dx'_1 dv'}{\vec{x}' \cdot \vec{x}' + a'^2 + f'_0} \right) \\ &+ d\vec{x}' d\vec{x}' + d\vec{z}' d\vec{z}', \end{aligned} \quad (\text{B.8})$$

$$B_{uv} = G_{uv}, \quad B_{vi} = -G_{vi}, \quad e^{-2\Phi} = 1 + \frac{Q'_5}{f'_0}.$$

Here rescaled coordinates and charges are defined by:

$$x'_i = x_i \frac{R\sqrt{V}}{g}, \quad u' = u \frac{R\sqrt{V}}{g}, \quad z'_1 = \frac{z_1 \sqrt{V}}{gR_1}, \quad (\text{B.9})$$

$$Q'_1 = \frac{Q_1 R^2 V}{g^2}, \quad Q'_5 = \frac{Q_5 R^2 V}{g^2}, \quad a' = \frac{a R \sqrt{V}}{g}, \quad (\text{B.10})$$

$$R' = \sqrt{V}, \quad V' = \frac{V}{gR_1^2}, \quad g' = \frac{VR}{gR_1}, \quad R'_1 = \frac{\sqrt{V}}{g}. \quad (\text{B.11})$$

Here  $f'_0 = f_0 \frac{R\sqrt{V}}{g}$  (not the derivative of  $f_0$ !), and in terms of the new coordinates it is given by

$$f'_0 = \left( (\vec{x}' \cdot \vec{x}')^2 + 2a'^2 (x'^2_3 + x'^2_4 - x'^2_1 - x'^2_2) + a'^4 \right)^{1/2}. \quad (\text{B.12})$$

The geometry (B.8) is an example of the chiral null model, we will discuss some properties of such models as well as their relations to the D1–D5 systems in the next appendix.



## C A chiral null model approach to D1-D5 solutions

In appendix B we have seen that under a chain of string dualities the rotating D1–D5 system (B.1) is mapped to the rotating fundamental string carrying momentum charge. The resulting solution (B.8) belongs to the class of the chiral null models [42]. Since chiral null models have been used in the past as a powerful tool for generating new solutions in supergravity, we will devote this appendix to studying such models and their transformations under the chain of dualities relating the fundamental string (B.8) and the D1–D5 system (B.1).

Let us first recall some of the properties of chiral null models [42]. The metric and matter fields for such models are given by:

$$\begin{aligned} ds^2 &= H'(\vec{x}', v') \left( -du' dv' + K'(\vec{x}', v') dv'^2 + 2A'_i(\vec{x}', v') dx'_i dv' \right) + d\vec{x}' \cdot d\vec{x}' + d\vec{z}' d\vec{z}', \\ B_{uv} &= -G_{uv} = \frac{1}{2} H'(\vec{x}', v'), \quad B_{vi} = -G_{vi} = -H'(\vec{x}', v') A'_i(\vec{x}', v'), \\ e^{-2\Phi} &= H'^{-1}(\vec{x}', v'). \end{aligned} \quad (\text{C.1})$$

Regarding  $A'_i$  as a gauge field we can construct the field strength  $\mathcal{F}_{ij} = A'_{j,i} - A'_{i,j}$ . The functions in the chiral null model are required satisfy the equations

$$\partial^2 H'^{-1} = 0, \quad \partial^2 K' = 0, \quad \partial_i \mathcal{F}^{ij} = 0. \quad (\text{C.2})$$

Here  $\partial^2$  is the Laplacian in the  $x'_i$  coordinates. Note that the indices  $i, j$  span the subspace  $\{x_i\}$  where the metric is just  $\delta_{ij}$ , and thus these indices are raised and lowered by this flat metric.

Note that the geometry (B.8) has a form of the chiral null model with

$$\begin{aligned} H'^{-1} &= 1 + \frac{Q'_5}{f'_0}, \quad K' = \frac{Q'_1}{f'_0}, \\ A'_1 &= \frac{2\sqrt{Q'_1 Q'_5} a' x'_2}{f'_0(f'_0 + \vec{x}' \cdot \vec{x}' + a'^2)}, \quad A'_2 = -\frac{2\sqrt{Q'_1 Q'_5} a' x'_1}{f'_0(f'_0 + \vec{x}' \cdot \vec{x}' + a'^2)}, \quad A'_3 = A'_4 = 0. \end{aligned} \quad (\text{C.3})$$

We now wish to develop an analogue of the chiral null models directly for the D1-D5 system; i.e., we wish to write supergravity solutions to the D1-D5 system in terms of functions that can be linearly superposed to generate new solutions. We can obtain such a formalism by applying dualities to the chiral null modes describing the FP system. But at some stage in these dualities we will have to perform a T-duality along the direction  $y'$ , so we look at FP solutions that are independent of  $y'$  to start with. This means that the functions  $H'$ ,  $K'$  and  $A'_i$  do not depend on  $v'$ , but are only functions of  $\vec{x}'$ .

First we make an S duality transformation to make the original string into the D1 brane carrying momentum. Then by applying T dualities along all directions of the torus  $(z_1, z_2, z_3, z_4)$  we produce the D5 brane carrying momentum:

$$ds^2 = -H^{1/2}(dt^2 - dy^2) + KH^{1/2}(dt - dy)^2 + 2H^{1/2}A_i dx^i(dt - dy)$$

$$+ H^{-1/2} d\vec{x}d\vec{x} + H^{1/2} d\vec{z}d\vec{z} \quad (\text{C.4})$$

$$e^{2\Phi} = H, \quad (\text{C.5})$$

$$C_{ti6789}^{(6)} = C_{iy6789}^{(6)} = -HA_i, \quad C_{ty6789}^{(6)} = H - 1 \quad (\text{C.6})$$

Since we will not use this metric later on, we are not writing a rescaling of coordinates which should be done to go from (C.1) to (C.4).

At this stage it is convenient to describe the RR fields not in terms of the six form (C.6), but in terms of the dual two form  $C^{(2)}$ . To construct this form we apply the electric–magnetic duality to (C.6). The field strength corresponding to (C.6) has following nonzero components:

$$G_{ti6789}^{(7)} = -G_{iy6789}^{(7)} = \partial_i(HA_j) - \partial_j(HA_i), \quad G_{ty6789}^{(7)} = -\partial_i H \quad (\text{C.7})$$

By applying the Hodge duality in ten dimensions we get a magnetically dual field strength:

$$G_{ijk}^{(3)} = -\epsilon^{ijkl} \partial_l H^{-1}, \quad (\text{C.8})$$

$$G_{tij}^{(3)} = -G_{ijy}^{(3)} = \epsilon^{ijkl} \partial_k A_l \quad (\text{C.9})$$

This field strength corresponds to the two–form RR field  $C_{\mu\nu}^{(2)}$ :

$$G_{\mu\nu\lambda}^{(3)} = 3\partial_{[\mu} C_{\nu\lambda]}^{(2)} \quad (\text{C.10})$$

So far we were only looking at configuration with no dependence upon  $t, y, z_i$ , so it is natural to require that  $C_{\nu\lambda}^{(2)}$  has the same property. This requirement is equivalent to fixing the gauge in  $C^{(2)}$ .

From the structure of  $G^{(3)}$  we conclude that the only nontrivial components of  $C^{(2)}$  are

$$C_{ij}^{(2)} \equiv C_{ij}, \quad C_{ti}^{(2)} = C_{iy}^{(2)} \equiv B_i \quad (\text{C.11})$$

and in terms of these new fields equations (C.8) become:

$$dC = -^* dH^{-1}, \quad dB = -^* dA. \quad (\text{C.12})$$

Here Hodge dual is taken with respect to the four dimensional space  $x^1, x^2, x^3, x^4$  with flat metric. Note that due to the equations of motion for the null chiral model (C.2):

$$d^* dH^{-1} = 0, \quad d^* dA = 0 \quad (\text{C.13})$$

the equations (C.12) can be integrated to give the forms  $C$  and  $B$ .

To summarize, the chiral null model dualized to the D5–P solution has metric (C.4) and dilaton field (C.5), but the RR fields can be described in two alternative ways. We either have a RR 6–form (C.6) or the RR 2–form

$$C_{ij}^{(2)} = C_{ij}, \quad C_{ti}^{(2)} = C_{iy}^{(2)} = B_i \quad (\text{C.14})$$

which is related to (C.6) by the electric magnetic duality (C.8).

We can now apply S duality followed by T dualities along  $y$  and  $z_1$  to transform the solution (C.4), (C.5), (C.14) into the F1-NS5 system. Application of another S duality gives the D1-D5 solution:

$$ds^2 = \sqrt{\frac{H}{1+K}} \left[ -(dt - A_i dx^i)^2 + (dy + B_i dx^i)^2 \right] + \sqrt{\frac{1+K}{H}} d\vec{x} \cdot d\vec{x} + \sqrt{H(1+K)} d\vec{z} \cdot d\vec{z} \quad (\text{C.15})$$

$$e^{2\Phi} = H(1+K), \quad C_{ti}^{(2)} = \frac{B_i}{1+K}, \quad C_{ty}^{(2)} = -\frac{K}{1+K},$$

$$C_{iy}^{(2)} = -\frac{A_i}{1+K}, \quad C_{ij}^{(2)} = C_{ij} \quad (\text{C.16})$$

The functions  $H$ ,  $K$  and  $A_i$  appearing in this solution have the same values as  $H'$ ,  $K'$  and  $A'_i$ :

$$H(\vec{x}) = H'(\vec{x}'), \quad K(\vec{x}) = K'(\vec{x}'), \quad A_i(\vec{x}) = A'_i(\vec{x}'), \quad (\text{C.17})$$

and the forms  $B_i$  and  $C_{ij}$  are defined by (C.12).

The functions  $H^{-1}$ ,  $K$ ,  $A_i$ ,  $B_i$  can be linearly superposed to give different solutions of the D1-D5 system. These functions depend only on  $\vec{x}$ ; further  $B_i$  is determined by  $A_i$  as described above.

## D Unbound solution.

We wish to construct a solution of the D1-D5 system which represents two D1-D5 bound states, with opposite angular momenta so that the total angular momentum is zero. We can either construct the solution from two strings in the FP system and perform dualities to the D1-D5 system, or work directly with the chiral null models derived for the D1-D5 system in appendix B and superpose two solutions. We will do the latter in this appendix.

Let us look at the simplest such superposition: we take a solution with  $Q_1, Q_5, a$  and add it to the solution with  $Q_1, Q_5, -a$  (actually we will take an average to preserve the asymptotic value of  $H$ ). The resulting system is described by

$$H^{-1} = 1 + \frac{Q_5}{f_0}, \quad K = \frac{Q_1}{f_0}, \quad A_i = 0 \quad (\text{D.1})$$

We can rewrite the result of superposition in terms of the original spherical coordinates  $r, \theta, \phi, \psi$  (see (B.5), (B.6)):

$$ds^2 = -\frac{f_0}{\sqrt{f_1 f_5}} (dt^2 - dy^2) + \sqrt{f_1 f_5} \left( \frac{dr^2}{r^2 + a^2} + d\theta^2 \right) + \sqrt{\frac{f_1}{f_5}} \sum_{i=1}^4 dz^i dz^i$$

$$+ \sqrt{\frac{f_1}{f_5}} \left( 1 + \frac{Q_5}{f_0} \right) \left[ r^2 \cos^2 \theta d\psi^2 + (r^2 + a^2) \sin^2 \theta d\phi^2 \right] \quad (\text{D.2})$$

$$e^{2\Phi} = \frac{f_5}{f_1}, \quad C_{ty}^{(2)} = -\frac{Q_1}{f_1}, \quad C_{\phi\psi}^{(2)} = \frac{Q_5(r^2 + a^2) \cos^2 \theta}{f_0}. \quad (\text{D.3})$$

To compare this solution with metrics for infinite throat and for the rotating D1–D5 branes we reduce the system (D.2) to six dimensions  $(t, r, \theta, \phi, \psi, y)$  and look at the resulting metric in the Einstein frame:

$$\begin{aligned} ds_E^2 &= e^{-\frac{4\Phi}{6-2}} ds_6^2 = -\frac{f_0}{\sqrt{f_1 f_5}} (dt^2 - dy^2) + \sqrt{f_1 f_5} \left( \frac{dr^2}{r^2 + a^2} + d\theta^2 \right) \\ &+ \frac{\sqrt{f_1 f_5}}{f_0} \left[ r^2 \cos^2 \theta d\psi^2 + (r^2 + a^2) \sin^2 \theta d\phi^2 \right] \end{aligned} \quad (\text{D.4})$$

We see that this metric has the form of a uniform throat only for  $r \gg a$ ; the geometry ends at  $r \sim a$ . Thus the resulting throat has a length that reflects the value of  $|a|$  of each component, rather than the total angular momentum (which is zero). We will examine the nature of the singularity at  $r = 0, \theta = \pi/2$  later on in appendix E.

## E Throat geometry for generic D1-D5 bound states

We wish to understand the supergravity solution corresponding to a general state out of the set of  $\sim e^{2\sqrt{2}\pi\sqrt{n_1 n_5}}$  Ramond ground states of the D1-D5 system. While we have seen in Appendix C how to write a metric using the idea of chiral null models directly for the D1-D5 system, we will proceed by first writing the metric for the FP system and then taking its dual. The reason for this is that we wish to make solutions that correspond to a single bound state of the D1-D5 system, rather than to a multicenter solution obtained from a collection of D1-D5 bound states. In the FP language a single bound state is given by the oscillations of a single string, and we start with these solutions.

Consider a single fundamental string carrying a momentum wave with profile  $\vec{G}(v')$ . Then the solution (C.1) with

$$\begin{aligned} H'^{-1}(\vec{x}', v') &= 1 + \frac{Q'}{|\vec{x}' - \vec{G}(v')|^2}, & K'(\vec{x}', v') &= \frac{Q' |\dot{\vec{G}}(v')|^2}{|\vec{x}' - \vec{G}(v')|^2} \\ A'_i(\vec{x}', v') &= -\frac{Q' \dot{G}_i(v')}{|\vec{x}' - \vec{G}(v')|^2} \end{aligned} \quad (\text{E.1})$$

describes a fundamental string located at  $\vec{x}' = \vec{G}(v')$ .

As in [34] we construct a superposition of such solutions by smearing over the coordinate  $y$  (or equivalently, by smearing over  $v$ ). This smearing arises because there are many closely spaced strands of the string in the space  $\vec{x}'$ , and in the classical limit their smoothed out effect is just obtained by superposing the continuous distribution given by the average over  $v'$ :

$$\langle H'^{-1} \rangle(\vec{x}') = \int_0^{L'} \frac{dv'}{L'} H'^{-1}(\vec{x}', v'), \quad \langle K' \rangle(\vec{x}') = \int_0^{L'} \frac{dv'}{L'} K(\vec{x}', v'),$$

$$\langle A'_i \rangle(\vec{x}') = \int_0^{L'} \frac{dv'}{L'} A'_i(\vec{x}', v'). \quad (\text{E.2})$$

Note that we obtain the solution (B.8) if we perform this smearing on the profile  $\vec{G}(v')$ :

$$G_1(v') = a' \cos(\omega v' + \alpha), \quad G_2(v') = a' \sin(\omega v' + \alpha), \quad G_3(v') = G_4(v') = 0, \quad (\text{E.3})$$

After duality transformations we get the D1-D5 solution (C.15) with coefficient functions

$$\langle H^{-1} \rangle(\vec{x}) = 1 + \frac{Q}{L} \int_0^L \frac{dv}{\sum (x_i - F_i(v))^2}, \quad (\text{E.4})$$

$$\langle K \rangle(\vec{x}) = \frac{Q}{L} \int_0^L \frac{\sum \dot{F}_i \dot{F}_i dv}{\sum (x_i - F_i(v))^2}, \quad (\text{E.5})$$

$$\langle A_i \rangle(\vec{x}) = -\frac{Q}{L} \int_0^L \frac{\dot{F}_i dv}{\sum (x_j - F_j(v))^2}. \quad (\text{E.6})$$

(We will not need the explicit form of  $\langle B_i \rangle$  and  $\langle C_{ij} \rangle$ .) From these expressions one can see that the functions  $\langle H^{-1} \rangle$ ,  $\langle K \rangle$ ,  $\langle A_i \rangle$  are regular everywhere, except at points where  $\vec{x} = \vec{F}(v)$  for some  $0 \leq v < L$ . Note that  $\vec{F}$  is related to  $\vec{G}$  by

$$\vec{F} = \frac{g}{R\sqrt{V}} \vec{G}. \quad (\text{E.7})$$

After dimensional reduction on the compact 4-manifold  $M$  we get the following 6-D Einstein metric for the D1-D5 system

$$ds_E^2 = \sqrt{\frac{H}{1+K}} \left[ -(dt - A_i dx^i)^2 + (dy + B_i dx^i)^2 \right] + \sqrt{\frac{1+K}{H}} d\vec{x} \cdot d\vec{x} \quad (\text{E.8})$$

with parameters given by (E.4)–(E.6). By translational invariance we can set

$$\int_0^L dv F_i(v) = 0. \quad (\text{E.9})$$

We will also assume that singularity is confined in the region with a typical size  $a$ , which means that

$$F_i(v) F_i(v) \leq a^2 \quad \text{for all } v \quad (\text{E.10})$$

Then for  $\vec{x}^2 \gg a^2$  we get:

$$\langle H^{-1} \rangle(\vec{x}) \approx 1 + \frac{Q}{\vec{x}^2}, \quad (\text{E.11})$$

$$\langle K \rangle(\vec{x}) \approx \frac{Q}{\vec{x}^2} \frac{1}{L} \int_0^L |\dot{\vec{F}}|^2 dv, \quad (\text{E.12})$$

$$\langle A_i \rangle(\vec{x}) = O((\vec{x}^2)^{-3/2}), \quad \langle B_i \rangle(\vec{x}) = O((\vec{x}^2)^{-3/2}) \quad (\text{E.13})$$

This leads to the leading approximation for the metric (E.8):

$$ds_E^2 \approx -\frac{1}{h}(dt^2 - dy^2) + h d\vec{x} d\vec{x}, \quad (\text{E.14})$$

where

$$h = \left[ \left(1 + \frac{Q}{\vec{x}^2}\right) \left(1 + \frac{\tilde{Q}}{\vec{x}^2}\right) \right]^{1/2}, \quad (\text{E.15})$$

$$\tilde{Q} = Q \frac{1}{L} \int_0^L |\dot{\vec{F}}|^2 dv. \quad (\text{E.16})$$

This solution can be trusted in the region  $\vec{x}^2 \gg a^2$ . We observe that in this approximation we get a geometry of the D1–D5 system with  $Q_5 = Q$  and  $Q_1 = \tilde{Q}$ .

We now wish to define a parameter  $\hat{a}$  which reduced to the parameter  $a$  for the special geometries (B.1) but for a general throat measures the effective size of the singularity (and thus determines the effective length of the throat). Thus we set

$$\hat{a} \equiv \left[ \frac{1}{L} \int_0^L |\vec{F}|^2 dv \right]^{1/2} \equiv [\langle |\vec{F}|^2 \rangle]^{1/2}. \quad (\text{E.17})$$

Taking into account the relation between charges (E.16), we can rewrite this expression as

$$\hat{a} = \sqrt{\frac{Q_1}{Q_5}} \left( \frac{\langle |\vec{F}|^2 \rangle}{\langle |\dot{\vec{F}}|^2 \rangle} \right)^{1/2}, \quad (\text{E.18})$$

Similarly, in the dual FP system we have

$$\hat{a}' = \sqrt{\frac{Q_P}{Q_w}} \left( \frac{\langle |\vec{G}|^2 \rangle}{\langle |\dot{\vec{G}}|^2 \rangle} \right)^{1/2}, \quad (\text{E.19})$$

where  $\vec{F}, \vec{G}$  are related as in (E.7) and

$$\hat{a}' = \frac{\hat{a} R \sqrt{V}}{g}, \quad \frac{Q_P}{Q_w} = \frac{Q_1}{Q_5}. \quad (\text{E.20})$$

In the FP system the string closes after  $n_w = n_5$  windings around the circle  $y'$  of length  $2\pi R'$ , so we may write

$$G_i(v) = \sum_{n=1}^{\infty} C_i^{(n)} \cos \left( \frac{nv}{n_5 R'} + \alpha_{n,i} \right) \quad (\text{E.21})$$

This leads us to the following averages:

$$\langle |\vec{G}|^2 \rangle = \frac{1}{2} \sum_{n=1}^{\infty} \sum_i \left( C_i^{(n)} \right)^2, \quad (\text{E.22})$$

$$\langle |\dot{\vec{G}}|^2 \rangle = \frac{1}{2(n_5 R')^2} \sum_{n=1}^{\infty} \sum_i n^2 \left( C_i^{(n)} \right)^2. \quad (\text{E.23})$$

If we define an “average harmonic”  $\bar{n}$  by

$$\bar{n} \equiv n_5 R' \left( \frac{\langle |\dot{\vec{G}}|^2 \rangle}{\langle |\vec{G}|^2 \rangle} \right)^{1/2}, \quad (\text{E.24})$$

then equation (E.19) becomes:

$$\hat{a}' = \sqrt{\frac{Q_P}{Q_w}} \frac{n_5 R'}{\bar{n}}. \quad (\text{E.25})$$

Using the relations (E.20) and (B.4) we find for the D1-D5 system

$$\hat{a} = \frac{\sqrt{n_1 n_5}}{\bar{n}} \frac{g}{R \sqrt{V}} \quad (\text{E.26})$$

We also define the generalization of the dimensionless parameter  $\gamma$  (eqn. (2.16)) for the D1-D5 system:

$$\hat{\gamma} \equiv \frac{\hat{a} R}{\sqrt{Q_1 Q_5}} \quad (\text{E.27})$$

which yields (using (B.4))

$$\hat{\gamma} = \frac{1}{\bar{n}} \quad (\text{E.28})$$

## F Wave equation near the singularity.

Let us look at the massless Klein–Gordon equation in the metric (E.8); the coefficient functions in the metric are given by (E.4) - (E.6). We will assume that the scalar field  $\Phi$  does not depend on  $y$  coordinate, and it depends on  $t$  only through the factor  $\exp(-i\omega t)$ :

$$\Psi(x_i, t, y) = \exp(-i\omega t) \tilde{\Psi}(x_i) \quad (\text{F.1})$$

Then the wave equation becomes:

$$-\omega^2 \left[ -\frac{1+K}{H} + A_i A_j \delta^{ij} \right] \Psi - i\omega \partial_i A_i \Psi - 2i\omega A_i \partial_i \Psi + \partial_i \partial^i \Psi = 0 \quad (\text{F.2})$$

From the expressions (E.4) - (E.6) one can see that the functions  $\langle H^{-1} \rangle(\vec{x})$ ,  $\langle K \rangle(\vec{x})$ ,  $\langle A_i \rangle(\vec{x})$  are regular everywhere, except at points where  $\vec{x} = \vec{F}(v)$  for some  $0 \leq v < L$ .

Consider the wave equation in the neighborhood of the point  $\vec{x}_0 = \vec{F}(v_0)$  on the singularity. We assume that (i) the singularity curve has no self-intersections, so that the direction of the curve is well defined at  $\vec{x}$  and (ii)  $|\dot{\vec{F}}(v_0)| \neq 0$ . Consider the 3-dimensional plane normal to the singular curve at  $\vec{x}_0$ , and parameterize the points in this plane by  $\vec{y}$ :

$$x_i = F_i(v_0) + y_i, \quad \dot{F}_i(v_0) y_i = 0. \quad (\text{F.3})$$

and we will look only at the displacements orthogonal to the singularity:

$$F_i(v_0)y_i = 0. \quad (\text{F.4})$$

Since  $y$  is a compact direction, all functions  $F_i(v)$  are periodic ( $F_i(v + L) = F_i(v)$ ). We then get

$$\partial_i \langle A_i \rangle = 0. \quad (\text{F.5})$$

Consider the potential term in (F.2)

$$\omega^2 \left[ \frac{1+K}{H} - A_i A_j \delta^{ij} \right] \Psi \quad (\text{F.6})$$

Each of the coefficient functions  $H^{-1}$ ,  $K$ ,  $A_i$  diverge as  $y^{-2}$  near the singular curve. It will be important for us that the combination occurring in the potential has a much softer divergence ( $\sim y^{-1}$ ) rather than the naively suggested  $\sim y^{-4}$ . We work this out below, and give an explanation of this softening in Appendix I.

We have

$$\begin{aligned} [1 + \langle K \rangle] \langle H^{-1} \rangle - \langle A_i \rangle \langle A_i \rangle = \\ \left( \frac{Q}{L} \right)^2 \int_0^L \int_0^L \frac{dv dv'}{(\vec{x} - \vec{F}(v))^2 (\vec{x} - \vec{F}(v'))^2} \frac{(\dot{\vec{F}}(v) - \dot{\vec{F}}(v'))^2}{2} \\ + \frac{Q}{L} \int_0^L \frac{(1 + \dot{\vec{F}}_i \dot{\vec{F}}_i) dv}{(\vec{x} - \vec{F}(v))^2} + 1 \end{aligned} \quad (\text{F.7})$$

We will consider only the curves without self intersection, then the main contribution to this integral comes from the vicinity of the point  $v_0$ . Let us evaluate the contribution from such vicinity to the first integral in (F.7):

$$\begin{aligned} I_1 &\equiv \left( \frac{Q}{L} \right)^2 \int_0^L \int_0^L \frac{dv dv'}{(\vec{x} - \vec{F}(v))^2 (\vec{x} - \vec{F}(v'))^2} \frac{(\dot{\vec{F}}(v) - \dot{\vec{F}}(v'))^2}{2} \\ &\approx 2 \left( \frac{Q}{L} \right)^2 \int_0^L \frac{dv (\dot{\vec{F}}(v) - \dot{\vec{F}}(v_0))^2}{\vec{y}^2 + (\vec{F}(v) - \vec{F}(v_0))^2} \int_0^L \frac{dv'}{\vec{y}^2 + [\dot{\vec{F}}(v_0)]^2 (v' - v_0)^2} \\ &\quad - 2 \left( \frac{Q}{L} \right)^2 \sum_i \int_0^L \frac{dv (\dot{F}_i(v) - \dot{F}_i(v_0))}{\vec{y}^2 + (\vec{F}(v) - \vec{F}(v_0))^2} \int_0^L \frac{dv' (\dot{F}_i(v') - \dot{F}_i(v_0))}{\vec{y}^2 + (\vec{F}(v) - \vec{F}(v_0))^2} \\ &\approx 2 \left( \frac{Q}{L} \right)^2 \frac{\pi}{|\dot{\vec{F}}(v_0)| \sqrt{\vec{y}^2}} \int_0^L \frac{dv (\dot{\vec{F}}(v) - \dot{\vec{F}}(v_0))^2}{(\vec{F}(v) - \vec{F}(v_0))^2} \\ &\quad - 2 \left( \frac{Q}{L} \right)^2 |\ddot{\vec{F}}(v_0)|^2 \left[ \int_0^L \frac{dv (v - v_0)}{\vec{y}^2 + (\vec{F}(v) - \vec{F}(v_0))^2} \right]^2 \end{aligned} \quad (\text{F.8})$$



The integral in the square brackets behaves as  $\log(\vec{y}^2)$ , and thus the leading asymptotics for  $I_1$  is

$$I_1 = \frac{C_1(v_0)}{|\vec{y}|} + o(|\vec{y}|^{-1}), \quad C_1(v_0) = 2 \left( \frac{Q}{L} \right)^2 \frac{\pi}{|\dot{\vec{F}}(v_0)|} \int_0^L \frac{dv (\dot{\vec{F}}(v) - \dot{\vec{F}}(v_0))^2}{(\vec{F}(v) - \vec{F}(v_0))^2} \quad (\text{F.9})$$

In the same fashion we will get the asymptotics of the second integral in (F.7):

$$I_2 \equiv \frac{Q}{L} \int_0^L \frac{(1 + \dot{\vec{F}}_i \dot{\vec{F}}_i) dv}{(\vec{x} - \vec{F}(v))^2} = \frac{C_2(v_0)}{|\vec{y}|} + o(|\vec{y}|^{-1}) \quad (\text{F.10})$$

$$C_2(v_0) = \frac{\pi Q}{L} (1 + |\dot{\vec{F}}(v_0)|^2) \frac{1}{|\dot{\vec{F}}(v_0)|} \quad (\text{F.11})$$

Thus we find that the expression (F.7) behaves near the singularity as

$$[1 + \langle K \rangle] \langle H^{-1} \rangle - \langle A_i \rangle \langle A_i \rangle \sim \frac{C(v_0)}{|\vec{y}|} \quad (\text{F.12})$$

(with  $C(v_0) > 0$ .)

To analyze the equation (F.2) we will also need the asymptotic behavior of  $A_i$ , which can be easily extracted from (E.6) and (F.10):

$$\langle A_i \rangle \sim \frac{C_3(v_0) \dot{\vec{F}}_i(v_0)}{|\vec{y}|}, \quad C_3(v_0) = -\frac{\pi Q}{L} \frac{1}{|\dot{\vec{F}}(v_0)|} \quad (\text{F.13})$$

In the four dimensional space  $x_1, x_2, x_3, x_4$  we have a vector  $\vec{y}$  which parameterizes a three dimensional subspace orthogonal to  $\dot{\vec{F}}(v_0)$  and coordinate  $z$  which measures the distance along the curve. The flat metric can be rewritten in terms of these four coordinates:

$$d\vec{x}d\vec{x} = d\vec{y}d\vec{y} + |\dot{\vec{F}}(z)|^2 dz^2 = dr^2 + r^2[d\theta^2 + \sin^2 \theta d\phi^2] + |\dot{\vec{F}}(z)|^2 dz^2. \quad (\text{F.14})$$

Here we have introduced the spherical coordinates  $r, \theta, \phi$  in the three dimensional space of  $\vec{y}$ .

Then substituting (F.12) and (F.13) into the equation (F.2), we get in the leading order in  $r = \sqrt{\vec{y} \cdot \vec{y}}$  and  $z$ :

$$\frac{C(z)\omega^2}{r} \Psi - \frac{2i\omega C_3(z)}{r} \partial_z \Psi + \frac{1}{|\dot{\vec{F}}(z)|} \partial_z \left( \frac{1}{|\dot{\vec{F}}(z)|} \partial_z \Psi \right) + r^{-2} \partial_r (r^2 \partial_r \Psi) + \frac{1}{r^2} \Delta_{\theta, \phi} \Psi = 0 \quad (\text{F.15})$$

The variables  $\theta$  and  $\phi$  in this equation separate and we will look for the solution in the form:

$$\Psi(t, r, z, \theta, \phi) = \exp(-i\omega t) Y_{lm}(\theta, \phi) \Phi(r, z), \quad (\text{F.16})$$

Let us first consider the case  $l > 0$ . In this case in the vicinity of  $r = 0$  we get an approximate equation:

$$r^{-2}\partial_r(r^2\partial_r\Phi) - \frac{l(l+1)}{r^2}\Phi = 0. \quad (\text{F.17})$$

This is a Schroedinger equation with repulsive potential and the particle is reflected from the barrier.

In the case of the S wave ( $l = m = 0$ ) it is convenient to introduce a new coordinate  $\rho = r^{1/2}$ . Then equation (F.15) becomes

$$C(z)\omega^2\Phi - 2i\omega C_3(z)\partial_z\Phi + \rho^2\partial_z\left(\frac{1}{|\dot{\vec{F}}(z)|}\partial_z\Phi\right) + \rho^{-3}\partial_\rho(\rho^3\partial_\rho\Phi) = 0. \quad (\text{F.18})$$

Assuming that  $z$  derivatives of  $\Phi$  are bounded:

$$|\partial_z\Phi| \leq B_1|\Phi|, \quad |\partial_z^2\Phi| \leq B_2|\Phi|, \quad (\text{F.19})$$

we get the asymptotic equation near  $\rho = 0$ :

$$\rho^{-3}\partial_\rho(\rho^3\partial_\rho\Phi) + \Lambda\Phi = 0 \quad (\text{F.20})$$

This is just the equation for the three dimensional spherical wave which moves in the constant potential. Such a wave reflects from  $\rho = 0$  after a finite number of oscillations and in a finite time. In the next Appendix we estimate the time spent near the singularity and show that it is less than (or at most comparable) to the time spent reaching  $r \sim a$  from the start of the throat.

## G Null geodesics near the singularity.

In this appendix we will look at null geodesics near the singularity, and estimate the time which a particle traveling along such geodesics spends in the vicinity of the singularity.

To analyze the geodesics we consider the Hamilton-Jacobi equation

$$g^{\mu\nu}\frac{\partial S}{\partial x^\mu}\frac{\partial S}{\partial x^\nu} = 0 \quad (\text{G.1})$$

in the background (E.8). We will assume that the particle does not move in the  $y$  direction:

$$\frac{\partial S}{\partial y} = 0. \quad (\text{G.2})$$

Then the Hamilton-Jacobi equation (G.1) becomes:

$$\left[-\frac{1+K}{H} + A_i A_j \delta^{ij}\right] \left(\frac{\partial S}{\partial t}\right)^2 + 2A_i \frac{\partial S}{\partial t} \frac{\partial S}{\partial x^i} + \frac{\partial S}{\partial x^i} \frac{\partial S}{\partial x^i} = 0. \quad (\text{G.3})$$

As in the Appendix F we will go from coordinates  $x^i$  to the coordinates  $z, r, \theta, \phi$  using (F.14). We will only study the geodesics which approach the singularity in the radial direction. For such geodesics the equation (G.3) becomes:<sup>9</sup>

$$\left[-\frac{1+K}{H} + A_i A_j \delta^{ij}\right] \left(\frac{\partial S}{\partial t}\right)^2 + \left(\frac{\partial S}{\partial r}\right)^2 = 0. \quad (\text{G.4})$$

Since coefficients in this equation do not depend on  $t$ , the solution has the form:

$$S(t, r) = \omega t + \tilde{S}(r). \quad (\text{G.5})$$

Near the singularity we can use the approximation (F.12), which allows us to rewrite (G.4) as

$$\frac{\partial \tilde{S}}{\partial r} \approx \omega \frac{\sqrt{C_1(z) + C_2(z)}}{\sqrt{r}}, \quad (\text{G.6})$$

where  $C_1(z)$  and  $C_2(z)$  are given by (F.9) and (F.11). For the generic singularity we have:

$$C_1(z) \approx 2 \left(\frac{Q}{L}\right)^2 \frac{\pi}{|\dot{\vec{F}}(z)|} L \frac{\langle |\dot{\vec{F}}|^2 \rangle}{\langle |\vec{F}|^2 \rangle} = \frac{2\pi Q_5}{L} \frac{1}{|\dot{\vec{F}}(z)|} \frac{Q_1}{\hat{a}^2} \quad (\text{G.7})$$

Here we have used (E.16), (E.17) and the definitions of  $Q_1$  and  $Q_5$ :  $Q_5 = Q$ ,  $Q_1 = \tilde{Q}$ . From eqn (E.16) we can see that if  $Q_1 \sim Q_5$ , then  $|\dot{\vec{F}}(z)| \sim 1$ , and comparing (F.11) with (G.7), we observe that  $C_1(z) \gg C_2(z)$  for  $\hat{a} \ll Q_1^{1/2}$ .

Equation (G.6) becomes

$$\frac{\partial \tilde{S}}{\partial r} \approx \frac{\omega}{\sqrt{r}} \left( \frac{2\pi}{L} \frac{1}{|\dot{\vec{F}}(z)|} \frac{Q_1 Q_5}{\hat{a}^2} \right)^{1/2} \quad (\text{G.8})$$

Integration of this equation gives the expression for the action (G.5)

$$S(t, r) = \omega t + 2\omega \sqrt{r} \left( \frac{2\pi}{L} \frac{1}{|\dot{\vec{F}}(z)|} \frac{Q_1 Q_5}{\hat{a}^2} \right)^{1/2} \quad (\text{G.9})$$

To get the travel time from  $r = r_0$  to  $r = 0$  we differentiate this action with respect to  $\omega$ :

$$\Delta t_{sing} = 2 \left( \frac{2\pi}{L} \frac{r_0}{|\dot{\vec{F}}(z)|} \frac{Q_1 Q_5}{\hat{a}^2} \right)^{1/2} = \frac{2}{\pi} \left( \frac{2\pi}{L} \frac{r_0}{|\dot{\vec{F}}(z)|} \right)^{1/2} \Delta t_{SUGRA}, \quad (\text{G.10})$$

---

<sup>9</sup>Note that  $A_i$  diverges at  $r = 0$  so there may be a residual contribution from the middle term in (G.3) even though the geodesic is radial to leading order as  $r \rightarrow 0$ . We do not expect this to qualitatively change the analysis, and so ignore such a potential contribution to (G.3).

where

$$\Delta t_{SUGRA} = \pi \frac{\sqrt{Q_1 Q_5}}{\hat{a}} \quad (\text{G.11})$$

is the travel time from the start of the throat to  $r = \hat{a}$  and back.

To determine the value of  $L$  we take the ratio of (E.18) and (E.19):

$$\frac{\hat{a}}{\hat{a}'} = \left( \frac{\langle |\vec{F}|^2 \rangle}{\langle |\vec{F}|^2 \rangle} \right)^{1/2} \left( \frac{\langle |\vec{G}|^2 \rangle}{\langle |\vec{G}|^2 \rangle} \right)^{1/2} = \frac{L}{L'}. \quad (\text{G.12})$$

At the last step we used the fact that the profiles  $\vec{F}$  and  $\vec{G}$  are related by a simple rescaling. Using the expression for  $\hat{a}'$  from (E.20) and the effective length for the FP system:  $L' = 2\pi n_5 R'$ , we get:

$$L = \frac{2\pi R' g n_5}{R \sqrt{V}} = \frac{2\pi g n_5}{R} = \frac{2\pi Q_5}{R} \quad (\text{G.13})$$

Substituting this value in (G.10) and replacing  $|\vec{F}(z)|$  by the average value

$$\langle |\vec{F}|^2 \rangle^{1/2} = \sqrt{\frac{Q_1}{Q_5}}, \quad (\text{G.14})$$

we get

$$\frac{\Delta t_{sing}}{\Delta t_{SUGRA}} = \frac{2}{\pi} \left( \frac{r_0 R}{(Q_1 Q_5)^{1/2}} \right)^{1/2} \quad (\text{G.15})$$

Taking  $r_0 \sim \hat{a}$  and using (E.27) and (E.28), we get:

$$\frac{\Delta t_{sing}}{\Delta t_{SUGRA}} \sim \frac{2}{\pi} \sqrt{\hat{\gamma}} = \frac{2}{\pi \sqrt{\bar{n}}} \quad (\text{G.16})$$

Since  $\bar{n} \geq 1$ , we see that the time spent near the singularity is of the order or smaller than the estimate  $\Delta t_{SUGRA}$ . Note that for the metrics (2.10) we have performed the exact computation for the travel time  $\Delta t_{SUGRA}$  (eqn. (3.7)); this time includes all effects of approaching the singularity and returning back.

## H Length of the singularity.

Consider the FP system, and look at the length of the singular curve in the space  $\vec{x}'$ . We assume that the coupling is weak, so that the metric is flat; the location of the string will give a localized singularity representing the physical location of the string. From the energy of oscillations we get:

$$\frac{n_P}{R'} = T \int |\dot{\vec{G}}|^2 dy' \quad (\text{H.1})$$

Then the length of the string is

$$D' = \int dy \sqrt{|\dot{\vec{G}}|^2} \leq L'^{1/2} \left[ \int |\dot{\vec{G}}|^2 dy' \right]^{1/2} = \sqrt{\frac{n_P L'}{R' T}} = 2\pi \sqrt{N \alpha'} \quad (\text{H.2})$$

where  $T = \frac{1}{2\pi\alpha'}$ . Note that equality is attained only if all the vibrations of the F string are in the same harmonic.

Let us map this to the D1-D5 system, and consider this system also at weak coupling so that spacetime is flat everywhere except the singularity. Then we get for the length of the singular curve

$$D = D' \frac{g \alpha'^{3/2}}{R \sqrt{V}} \leq 2\pi \sqrt{N \alpha'} \frac{g \alpha'^{3/2}}{R \sqrt{V}} = 2\sqrt{2} \frac{\sqrt{N G^{(6)}}}{R} \quad (\text{H.3})$$

We can then write for the ‘area’ occupied by the singularity in the  $\vec{x}, y$  space

$$Area = 2\pi R D \leq 4\pi \sqrt{2} \sqrt{N G^{(6)}}, \quad (\text{H.4})$$

where we again note that equality is attained only if all the component strings in the microstate are of equal length (this is equivalent to all vibrations being in the same harmonic for the dual FP system).

## I Singularity curves having self intersections

Consider the potential term (F.6) that we found in the scalar wave equation near the singular curve of the D1-D5 geometry. We had found that this term was much less singular than would appear from the behavior of its individual factors. This softening of the singularity was essential for the fact that the wave reflects back in a finite time from the singularity. Let us look at the FP system, and investigate the essential reason for this softening as well as the situations where the wave equation may become more singular.

Suppose we have a single strand of a fundamental string oscillating with some profile  $\vec{G}(v')$ . Then we find, using (E.1), that

$$\mathcal{P} \equiv K'(H'^{-1} - 1) - A'_i A'_j \delta^{ij} = 0 \quad (\text{I.1})$$

If however we have two strands of the string (whether joined into one string or arising from two separate strings) then

$$\mathcal{P} = \frac{Q'_1 Q'_2}{|\vec{x}' - \vec{G}_1(v')|^2 |\vec{x}' - \vec{G}_2(v')|^2} |\vec{G}_1(v') - \vec{G}_2(v')|^2, \quad (\text{I.2})$$

which is nonzero unless the profiles  $\vec{G}_1(v')$  and  $\vec{G}_2(v')$  are the same.

The quantity  $\mathcal{P}$  differs from the potential (F.6) only by terms that are comparatively nonsingular. Now consider the multiwound string. If the singular curve it produces in the space  $\vec{x}'$  has no self-intersections, then neighboring strands along this curve have almost the same profile  $\vec{G}(v')$ . In that case the quantity (I.2) is comparatively regular, and thus we see that the softening of the potential in the wave equation can be traced back to the vanishing of  $\mathcal{P}$  for a single strand.

But if the singular curve has self-intersections, then at the same point in the space  $\vec{x}'$  we have strands with quite different profiles  $G_1(v'), G_2(v')$ . The denominators in (I.2) now cause  $\mathcal{P}$  to be large, and the potential in the wave equation is correspondingly more singular.

Since the singular curve is a 1-D hypersurface in the 4-D space  $\vec{x}'$ , the generic singular curve has no self intersections. But since simple examples may actually have such intersections, we examine two such cases in this Appendix.

(i) The ‘unbound state’ solution (D.2) was constructed by superposing two bound states, each of which had a singularity on the same circle of radius  $a$ . Let us look at the dual FP system. Since the rotation was oppositely directed in the two components, we find at each point along the singular curve a pair of strands with different profiles  $G_1(v'), G_2(v')$ . Thus each point of the singular curve gives a more singular potential in the wave equation than the generic  $\sim 1/|\vec{y}|$  (eqn. (F.15)).

We now find that geodesics that go radially into any point with  $r = 0, \theta = \pi/2$  do not return back in a finite time  $t$ . The divergence in this time of flight is however only logarithmic: if we separate the two components of the D1-D5 solution by a distance  $\delta r$  then the time of flight to the singularity again becomes finite and of order  $\sim \Delta t_{CFT} \log \frac{\delta r}{a}$ . But now note that each bound state in the solution had some mass  $M$ , and thus can be localized in the space  $\vec{x}$  only to an accuracy  $|\delta \vec{x}| \sim 1/M$ . If we set  $Q_1 \sim Q_5$  for the moment, and work out the effect of this fluctuation, then we find that

$$\Delta t_{SUGRA} \sim \Delta t_{CFT} \log j \quad (\text{I.3})$$

where  $j$  is the angular momentum of each of the bound states in the solution. We will not explore the meaning of this logarithm further, but just note that such logs have appeared before in relating CFT and supergravity quantities [43].

(ii) As a second example we write down an explicit solution for the single bound state where the singularity is a straight line: this will be the limiting case where the ellipse in figure 5 degenerates and the angular momentum becomes zero.

Consider the string of the FP system oscillating in the direction  $x_1$ :

$$G_1(v') = a' \cos(\omega v' + \alpha), \quad G_2(v') = G_3(v') = G_4(v') = 0. \quad (\text{I.4})$$

Averaging over  $\alpha$  in the usual manner we get the classical solution (C.15) with coefficient functions

$$H^{-1} = \left( 1 + \frac{Q_5}{2r} \left[ \frac{2(r^2 - z^2 + a^2) + 2\sqrt{(r^2 - z^2 + a^2)^2 + 4z^2r^2}}{(r^2 - z^2 + a^2)^2 + 4z^2r^2} \right]^{1/2} \right) \quad (\text{I.5})$$

$$K = \frac{Q_1}{ra^2} \left( -2r + \left[ 2(r^2 - z^2 + a^2) + 2\sqrt{(r^2 - z^2 + a^2)^2 + 4z^2r^2} \right]^{1/2} \right) \quad (\text{I.6})$$

$$A_i = 0. \quad (\text{I.7})$$

At each point of the singularity we have two differently moving strands of the string arising from the two sides of the degenerating ellipse. Correspondingly we find that there is a logarithmic divergence in the time of flight to each point on the singularity; in addition there is a stronger singularity at the endpoints  $x_1 = \pm a$  since here  $|\dot{\vec{G}}(v')|$  vanishes as well, and so the density of points along the singular curve (4.17) diverges .

## References

- [1] O. Aharony, S. S. Gubser, J. Maldacena, H. Ooguri and Y. Oz, Phys. Rept. **323**, 183 (2000), hep-th/9905111.
- [2] S. R. Das and S. D. Mathur, Ann. Rev. Nucl. Part. Sci. **50**, 153 (2000), gr-qc/0105063.
- [3] S. W. Hawking, Commun. Math. Phys. **43**, 199 (1975).
- [4] A. Strominger and C. Vafa, Phys. Lett. B **379**, 99 (1996), hep-th/9601029.
- [5] C. G. Callan and J. M. Maldacena, Nucl. Phys. B **472**, 591 (1996), hep-th/9602043.
- [6] S. R. Das and S. D. Mathur, Nucl. Phys. B **478**, 561 (1996), hep-th/9606185.
- [7] S. R. Das and S. D. Mathur, Nucl. Phys. B **482**, 153 (1996), hep-th/9607149.
- [8] J. Maldacena, Adv. Theor. Math. Phys. **2**, 231 (1998), Int. J. Theor. Phys. **38**, 1113 (1998), hep-th/9711200.
- [9] O. Coussaert and M. Henneaux, Phys. Rev. Lett. **72**, 183 (1994), hep-th/9310194.
- [10] J. Maldacena and A. Strominger, JHEP **9812**, 005 (1998), hep-th/9804085.
- [11] G. T. Horowitz and H. Ooguri, Phys. Rev. Lett. **80**, 4116 (1998), hep-th/9802116.
- [12] O. Lunin and S. D. Mathur, hep-th/0107113.
- [13] S. S. Gubser, I. R. Klebanov and A. M. Polyakov, Phys. Lett. B **428**, 105 (1998), hep-th/9802109.
- [14] E. Witten, Adv. Theor. Math. Phys. **2**, 253 (1998), hep-th/9802150.
- [15] V. Balasubramanian, P. Kraus and A. E. Lawrence, Phys. Rev. D **59**, 046003 (1999), hep-th/9805171.

- [16] V. Balasubramanian, J. de Boer, E. Keski-Vakkuri and S. F. Ross, Phys. Rev. D **64**, 064011 (2001), hep-th/0011217;  
J. Maldacena and L. Maoz, hep-th/0012025.
- [17] D. Z. Freedman, S. D. Mathur, A. Matusis and L. Rastelli, Nucl. Phys. B **546**, 96 (1999), hep-th/9804058;  
E. D'Hoker, S. D. Mathur, A. Matusis and L. Rastelli, Nucl. Phys. B **589**, 38 (2000), hep-th/9911222.
- [18] S. D. Mathur, Int. J. Mod. Phys. A **15**, 4877 (2000), gr-qc/0007011.
- [19] N. Seiberg and E. Witten, JHEP **9904**, 017 (1999), hep-th/9903224.
- [20] J. de Boer, JHEP **9905**, 017 (1999), hep-th/9812240.
- [21] R. Dijkgraaf, Nucl. Phys. B **543**, 545 (1999), hep-th/9810210.
- [22] F. Larsen and E. J. Martinec, JHEP **9906**, 019 (1999) hep-th/9905064.
- [23] J. R. David, G. Mandal and S. R. Wadia, Nucl. Phys. B **564**, 103 (2000), hep-th/9907075.
- [24] R. Dijkgraaf, E. Verlinde and H. Verlinde, Nucl. Phys. B **500**, 43 (1997), hep-th/9703030.
- [25] A. Jevicki, M. Mihailescu and S. Ramgoolam, Nucl. Phys. B **577**, 47 (2000), hep-th/9907144.
- [26] O. Lunin and S. D. Mathur, hep-th/0103169.
- [27] M. Cvetič and F. Larsen, Phys. Rev. D **56**, 4994 (1997), hep-th/9705192.
- [28] J. Maldacena and A. Strominger, Phys. Rev. D **55**, 861 (1997), hep-th/9609026.
- [29] J. M. Maldacena and L. Susskind, Nucl. Phys. B **475**, 679 (1996), hep-th/9604042.
- [30] A. W. Peet and J. Polchinski, Phys. Rev. D **59**, 065011 (1999), hep-th/9809022.
- [31] J. Maldacena and A. Strominger, Phys. Rev. D **56**, 4975 (1997), hep-th/9702015.
- [32] S. S. Gubser, Phys. Rev. D **56**, 4984 (1997), hep-th/9704195.
- [33] S. D. Mathur, Nucl. Phys. B **514**, 204 (1998), hep-th/9704156.
- [34] O. Lunin and S. D. Mathur, Nucl. Phys. B **610**, 49 (2001), hep-th/0105136.
- [35] S. R. Das and S. D. Mathur, Phys. Lett. B **375**, 103 (1996), hep-th/9601152.



- [36] J. Michelson and A. Strominger, JHEP **9909**, 005 (1999), hep-th/9908044;  
J. Gutowski and G. Papadopoulos, Phys. Rev. D **62**, 064023 (2000), hep-th/0002242.
- [37] S. R. Das and S. D. Mathur, Phys. Lett. B **365**, 79 (1996), hep-th/9507141.
- [38] S. D. Mathur, Nucl. Phys. B **529**, 295 (1998), hep-th/9706151.
- [39] D. A. Lowe, J. Polchinski, L. Susskind, L. Thorlacius and J. Uglum, Phys. Rev. D **52**, 6997 (1995), hep-th/9506138.
- [40] A. Dhar, G. Mandal and S. R. Wadia, Phys. Lett. B **388**, 51 (1996), hep-th/9605234.
- [41] T. Banks, M. R. Douglas, G. T. Horowitz and E. J. Martinec, hep-th/9808016.
- [42] G. T. Horowitz and A. A. Tseytlin, Phys. Rev. D **51**, 2896 (1995), hep-th/9409021;  
A. A. Tseytlin, Phys. Lett. B **381**, 73 (1996) hep-th/9603099.
- [43] I. R. Klebanov and S. D. Mathur, Nucl. Phys. B **500**, 115 (1997), hep-th/9701187.
- [44] S. R. Das and S. P. Trivedi, Phys. Lett. B **445**, 142 (1998), hep-th/9804149;  
S. S. Gubser, A. Hashimoto, I. R. Klebanov and M. Krasnitz, Nucl. Phys. B **526**,  
393 (1998), hep-th/9803023.